Oxidative condensation/esterification of furfural with ethanol using preformed Au colloidal nanoparticles. Impact of stabilizer and heat treatment protocols on catalytic activity and stability

(Article begins on next page)

31 January 2025

Highlights

- Oxidative condensation of furfural with ethanol using preformed Au colloidal nanoparticles.

- Impact of stabilizers (PVA and PVP) and heat treatment protocols on catalytic activity and stability.

- Effect of Au particle size in terms of catalytic activity and yield of products.

- Tuning the surface coverage of Au for controlling catalytic activity.

Oxidative condensation of furfural with ethanol using preformed Au colloidal nanoparticles. Impact of stabilizer and heat treatment protocols on catalytic activity and stability

Eleonora Monti[1,2], Alessia Ventimiglia[1,2], Carolina Alejandra Garcia Soto[1,2], Francesca Martelli[1,2], Elena Rodríguez-Aguado[3], Juan Antonio Cecilia[3*], Pedro Maireles-Torres[3], Francesca Ospitali[1,2], Tommaso Tabanelli[1,2], Stefania Albonetti[1,2], Fabrizio Cavani[1,2], Nikolaos Dimitratos[1,2]*

[1]Dipartimento di Chimica Industriale "Toso Montanari", Alma Mater Studiorum Università di Bologna, Viale Risorgimento 4, 40126 Bologna, Italy
[2]Center for Chemical Catalysis-C3, Alma Mater Studiorum Università di Bologna, Viale Risorgimento 4, 40136 Bologna, Italy
[3]Departamento de Química Inorgánica, Cristalografía y Mineralogía (Unidad Asociada al ICP-CSIC), Facultad de Ciencias, Universidad de Málaga, Campus de Teatinos, 29071 Málaga, Spain
*Correspondence: nikolaos.dimitratos@unibo.it (N.D.); jacecilia@uma.es (J.A.C.)

Supplementary information
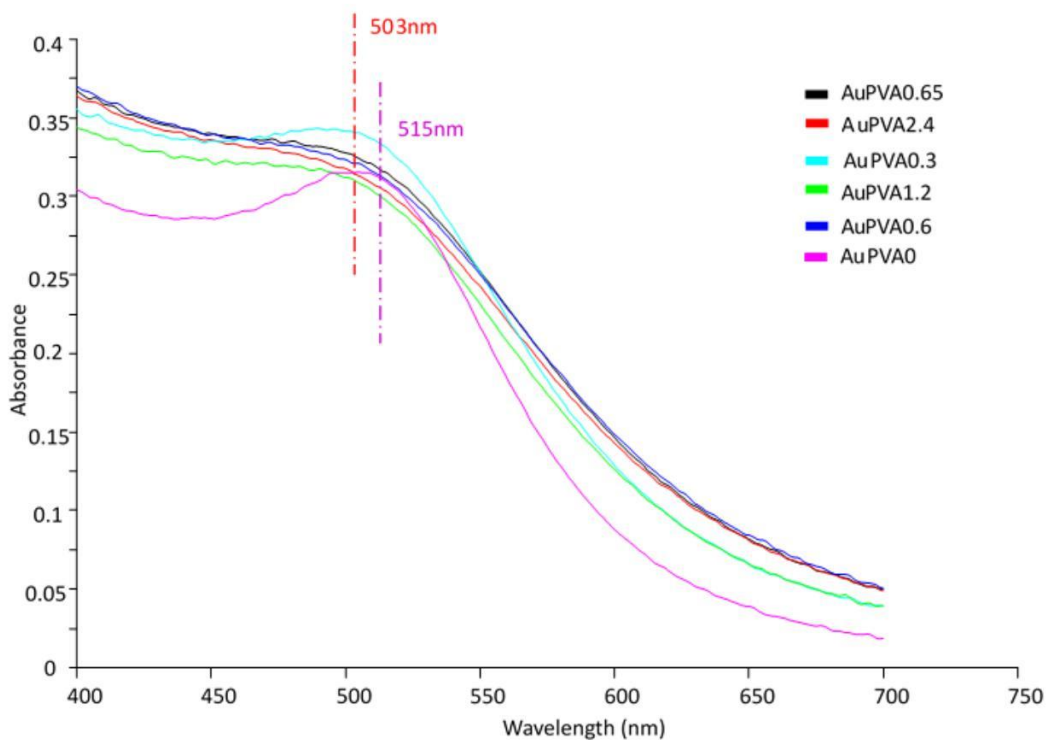
Figure S1. UV-Vis spectra of Au colloidal solutions with different PVA:Au weight ratio.
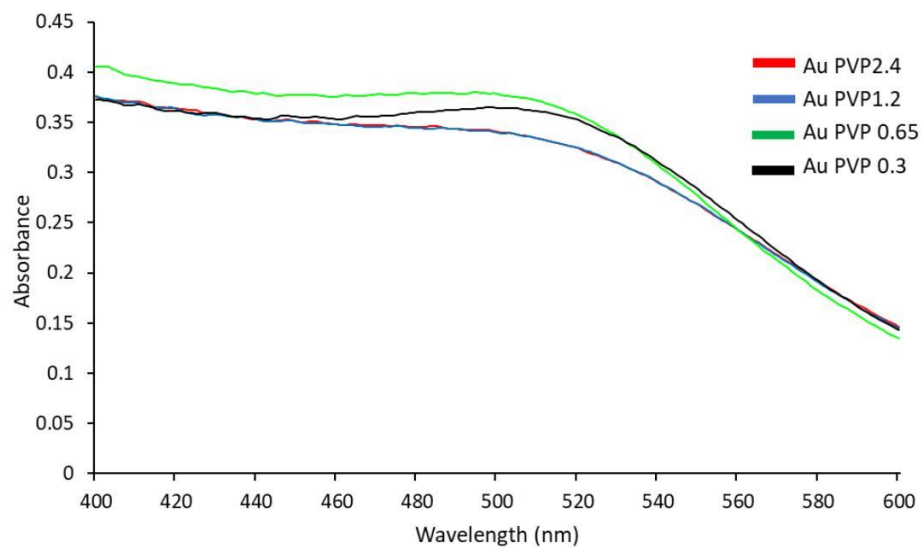
Figure S2. UV-Vis spectra for Au/AC PVP series after 25min from the addition of NaBH$_4$.
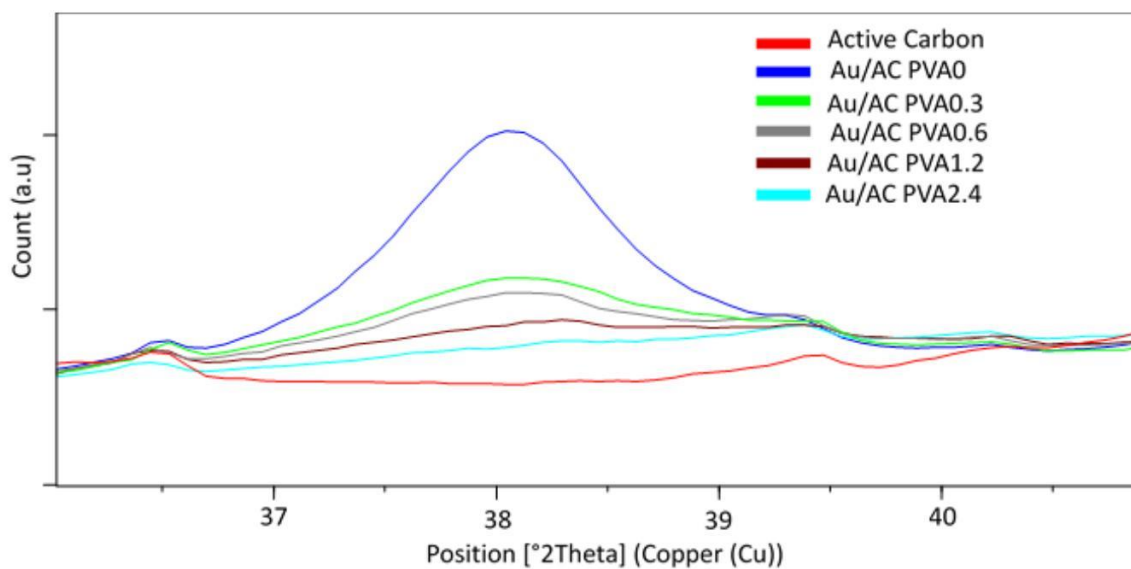
Figure S3. XRD patterns of activated carbon and Au/AC samples with different PVA:Au weight ratio.

Table S1. Mean crystallite size for Au/AC using PVA with different PVA:Au weight ratio.

Catalyst	Mean crystallite size (nm)
Au/AC PVA0	6.4
Au/AC PVA0.3	3.6
Au/AC PVA0.6	3.1
Au/AC PVA1.2	2.6
Au/AC PVA2.4	2.2

Table S2. Mean crystallite size for Au/AC using PVP with different PVP:Au weight ratio.

Catalyst	Mean crystallite size (nm) by XRD
Au/AC PVP0.3	6.7
Au/AC PVP0.65	6.4
Au/AC PVP 1.2	8.2
Au/AC PVP2.4	8.1

- **Au/AC (PVA/Au = 0.3)**
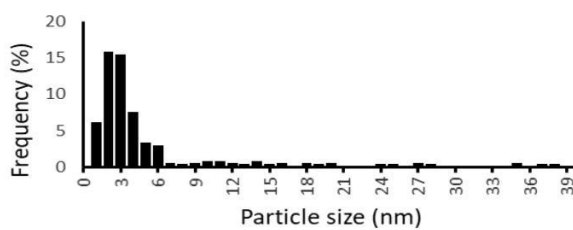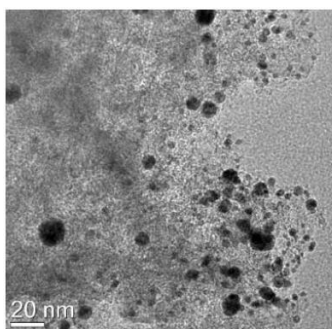
- **Au/AC (PVA/Au = 0.6)**
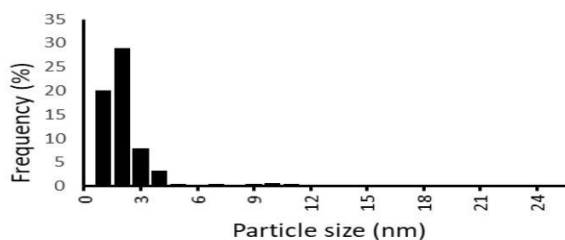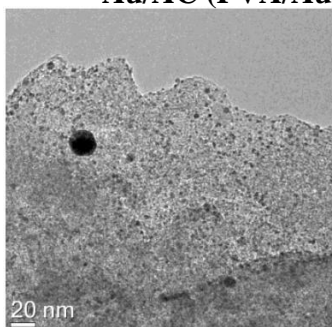
- **Au/AC (PVA/Au = 1.2)**
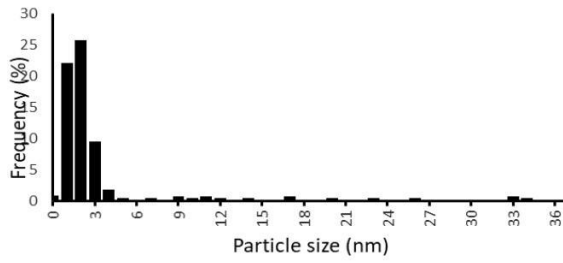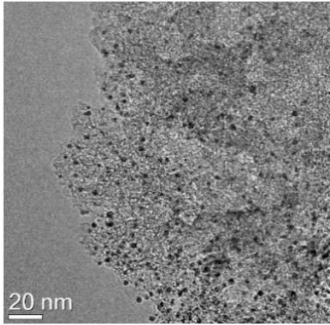
- **Au/AC (PVA/Au = 2.4)**
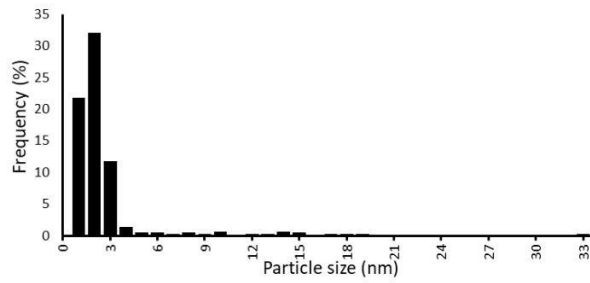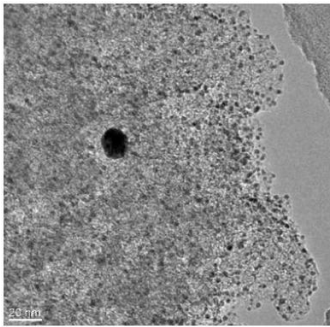
Figure S4. TEM images and particle size distributions of Au/AC synthesized using PVA with different PVA:Au weight ratio.

- **Au/AC (PVP/Au = 0.3)**
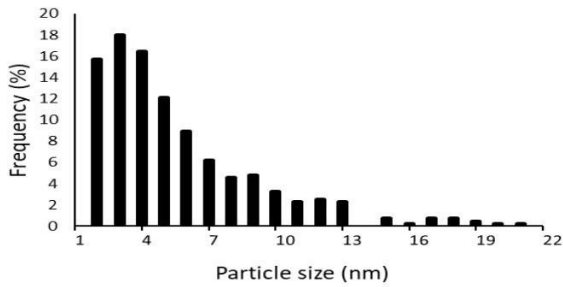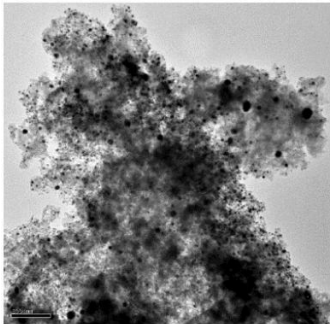
- **Au/AC (PVP/Au = 0.65)**
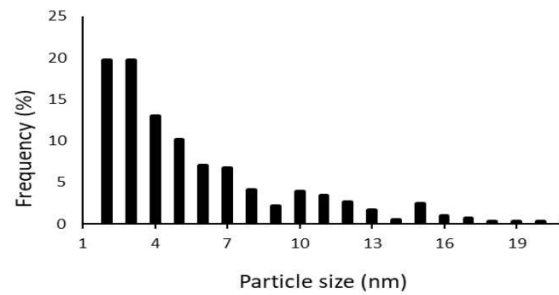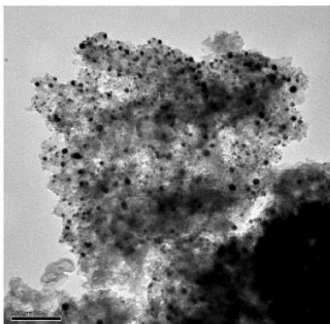
- **Au/AC (PVP/Au = 1.2)**
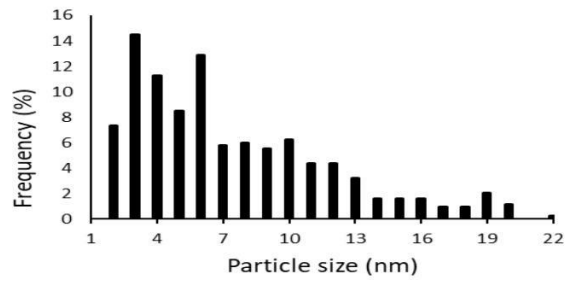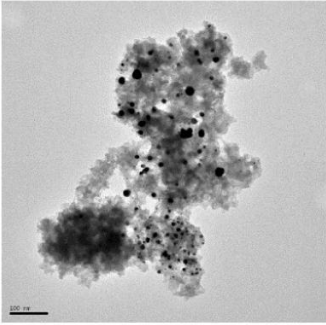
- **Au/AC (PVP/Au = 2.4)**
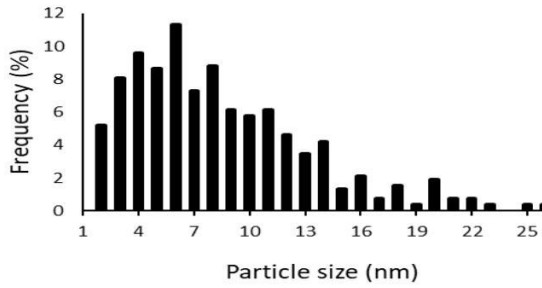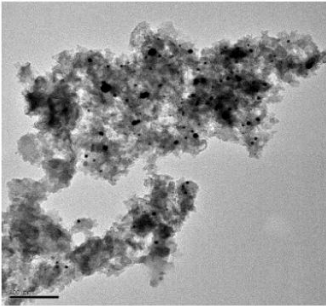
Figure S5. TEM images and particle size distributions of Au/AC synthesized using PVP with different PVA:Au weight ratio.
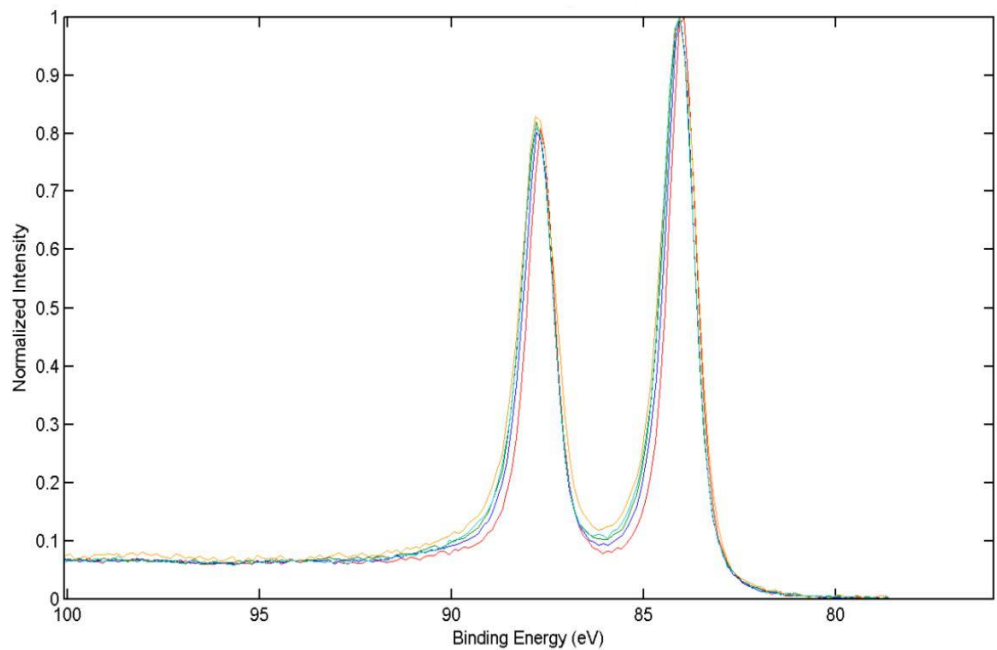
Figure S6. XPS spectra for Au/AC using PVA with different PVA:Au weight ratio.
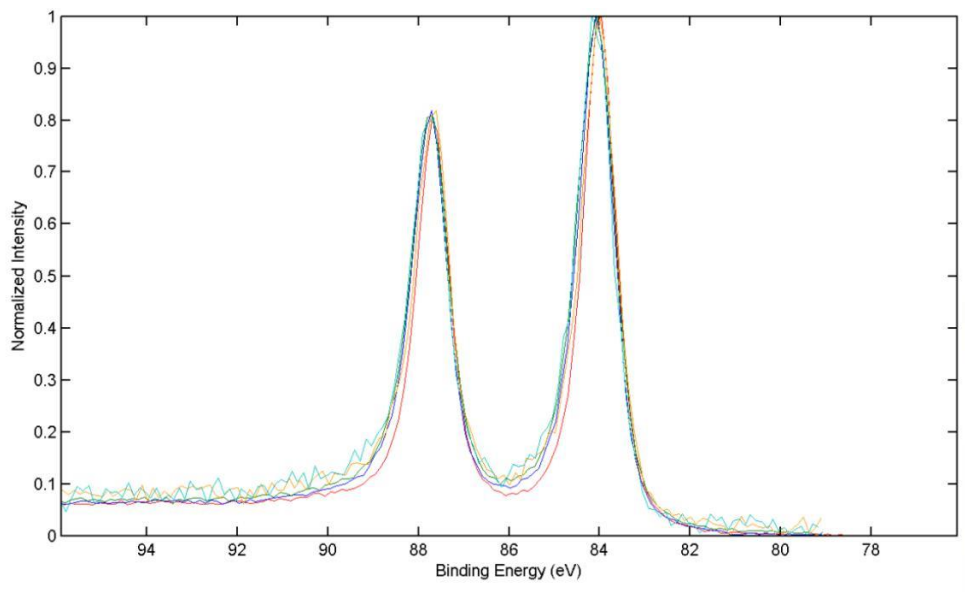
Figure S7. XPS spectra for Au/AC using PVP with different PVP:Au weight ratio (label "Au/AC PVP06" is the catalyst with PVP/Au=0.65 weight ratio).

Table S3. XPS data for supported Au nanoparticles using PVA and PVP with different polymer to Au weight ratio.

Samples	Au 4f$_{7/2}$ BE [eV]	Surface atomic concentration [%]			Surface Au/C atomic ratio
		Au 4f	C 1s	N 1s	
Au/AC 0	84.0	2.61	91.64	-	0.028
Au/AC PVA0.3	84.1	3.48	87.52	-	0.039
Au/AC PVA0.6	84.1	2.80	85.80	-	0.033
Au/AC PVA1.2	84.1	2.40	82.55	-	0.029
Au/AC PVA2.4	84.1	1.81	82.53	-	0.022
Au/AC PVP0.3	84.0	1.43	90.94	2.10	0.016
Au/AC PVP0.65	84.0	1.17	88.69	3.25	0.013
Au/AC PVP1.2	84.0	0.15	90.81	2.90	0.0016
Au/AC PVP2.4	84.1	0.12	89.53	3.60	0.0013

Table S4. Mean crystallite size and mean particle size of Au/AC heat-treated obtained by XRD and TEM analysis.

Catalyst	Mean crystallite size (nm) by XRD	Mean particle size (nm) by TEM± Standard Deviation
Au/AC no treat	3.1	2.7±1.6
Au/AC HT120	2.9	4.2±2.3
Au/AC HT200	4.1	4.9±2.9
Au/AC HT250	7.5	5.8±4.1

Table S5. Au atomic percentage on surface, surface atomic ratio Au/C and mean particle size for Au/AC HT series.

Samples	Au on surface (at%)	Surface atomic ratio Au/C	Mean particle size (nm) (TEM)
Au/AC no treat	2.8	0.033	2.7
Au/AC HT120	2.79	0.032	4.2
Au/AC HT200	2.66	0.029	4.9
Au/AC HT250	1.14	0.012	5.8

Table S6. Reproducibility of catalytic tests.

	Conversion (Fur)	Yield (EtFur)	Yield (Fur-2-Acr)
Test 1	44	12	31
Test 2	48	10	33
Test 3	49	10	26
Average	47	11	30
Standard Deviation	2	1	4
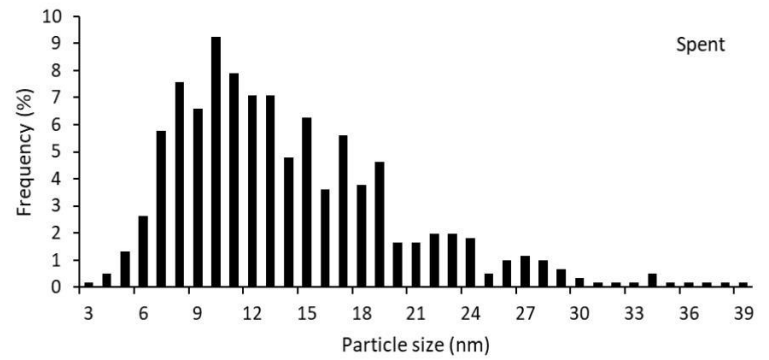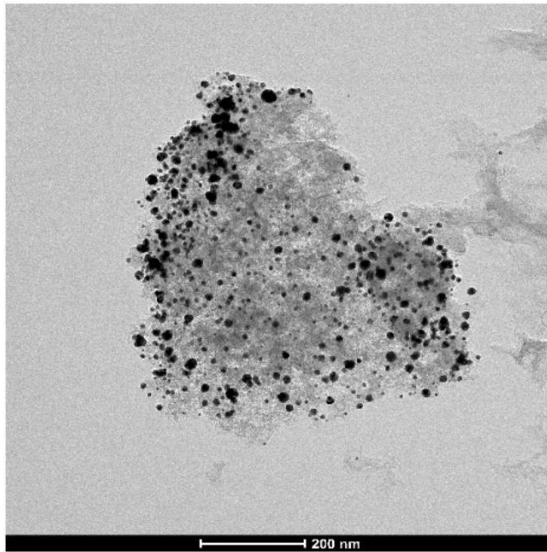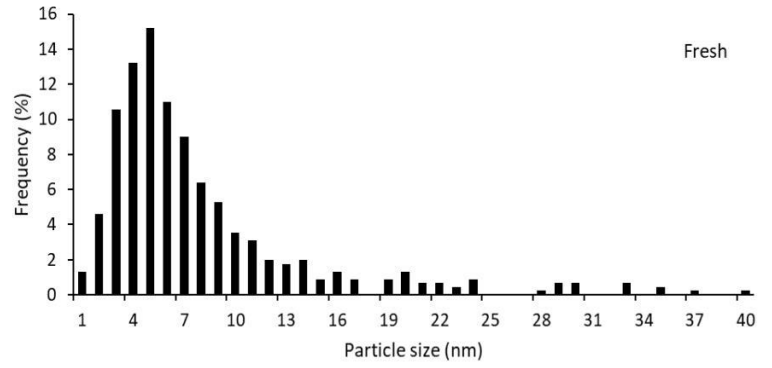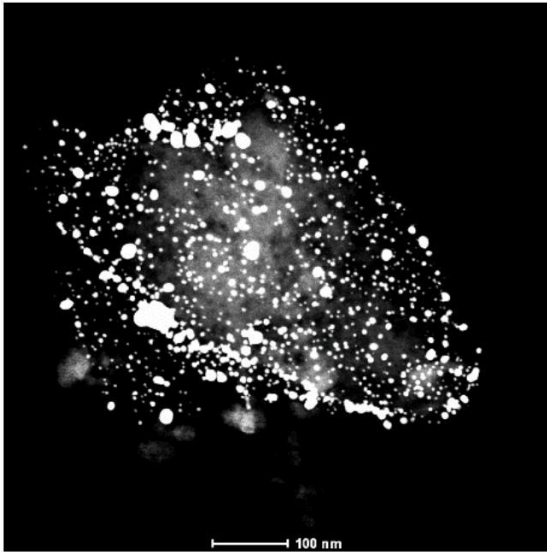
Figure S8. TEM/STEM analysis and particle size distribution of Au/AC PVA0 fresh and used catalysts.
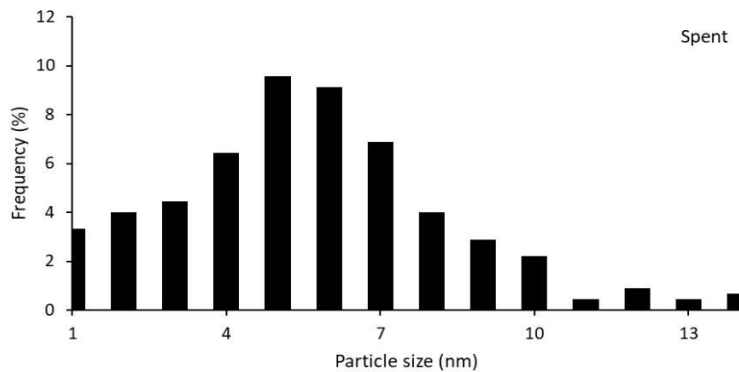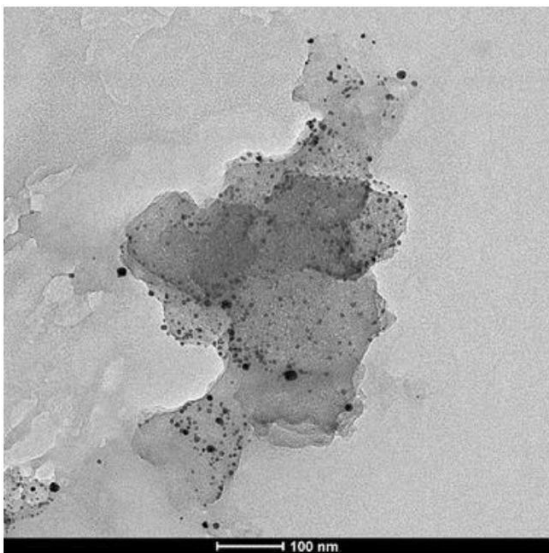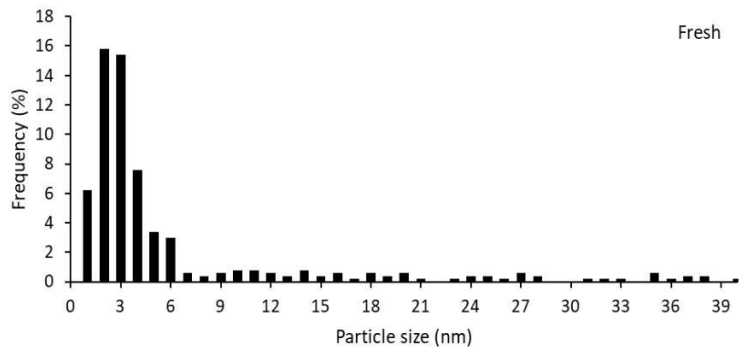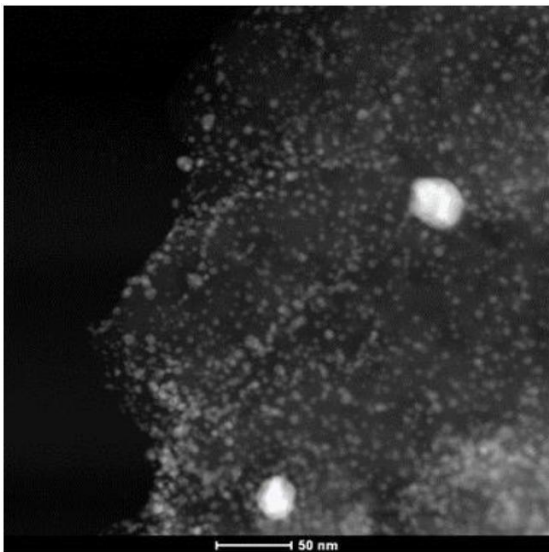
Figure S9. TEM/STEM analysis and particle size distribution of Au/AC PVA0.3 fresh and used catalysts.
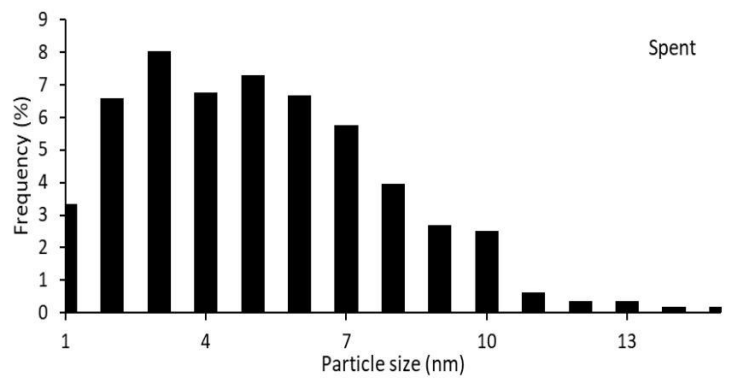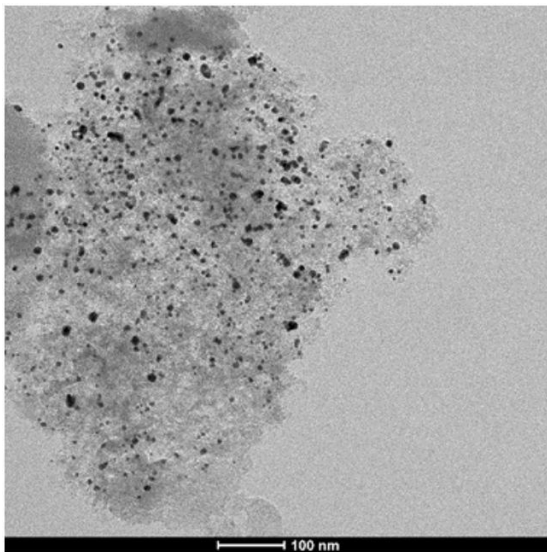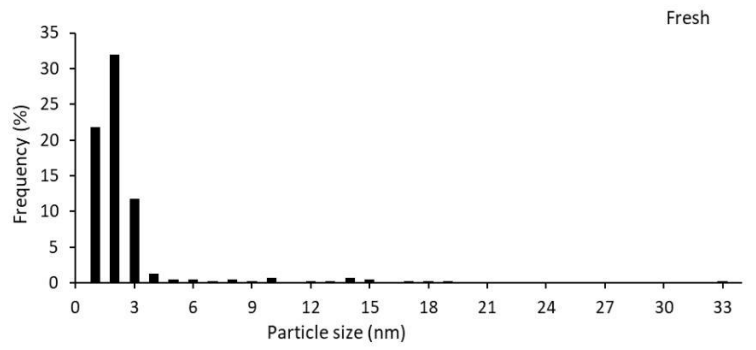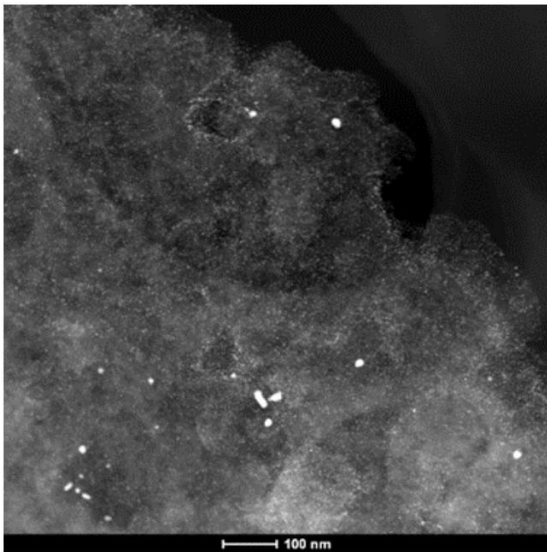
Figure S10. TEM/STEM analysis and particle size distribution of Au/AC PVA2.4 fresh and used catalysts.

Figure S11. Samples of reaction solution after catalytic tests as a function of reaction temperature.

Declaration of interests

☒The authors declare that they have no known competing financial interests or personal relationships that could have appeared to influence the work reported in this paper.

☐The authors declare the following financial interests/personal relationships which may be considered as potential competing interests:

Oxidative condensation/esterification of furfural with ethanol using preformed Au colloidal nanoparticles. Impact of stabilizer and heat treatment protocols on catalytic activity and stability

Eleonora Monti[1,2], Alessia Ventimiglia[1,2], Carolina Alejandra Garcia Soto[1,2], Francesca Martelli[1,2], Elena Rodríguez-Aguado[3], Juan Antonio Cecilia[3*], Pedro Maireles-Torres[3], Francesca Ospitali[1,2], Tommaso Tabanelli[1,2], Stefania Albonetti[1,2], Fabrizio Cavani[1,2], Nikolaos Dimitratos[1,2]*

[1]Dipartimento di Chimica Industriale "Toso Montanari", Alma Mater Studiorum Università di Bologna, Viale Risorgimento 4, 40126 Bologna, Italy
[2]Center for Chemical Catalysis-C3, Alma Mater Studiorum Università di Bologna, Viale Risorgimento 4, 40136 Bologna, Italy
[3]Departamento de Química Inorgánica, Cristalografía y Mineralogía (Unidad Asociada al ICP-CSIC), Facultad de Ciencias, Universidad de Málaga, Campus de Teatinos, 29071 Málaga, Spain
*Correspondence: nikolaos.dimitratos@unibo.it (N.D.); jacecilia@uma.es (J.A.C.)

Abstract: The oxidative condensation of furfural and ethanol has been studied using supported gold colloidal nanoparticles. The influence of the nature of stabilizer (polyvinylalcohol, polyvinylpyrrolidone), the choice of thermal treatment and washing for removing the stabilizer, on the catalytic performance has been evaluated. Variation of the mean gold particle size and surface coverage of the gold nanoparticles onto the support surface were achieved by modifying the stabilizer to Au weight ratio. Thus, the mean gold particle size was varied in the range of 3-8 nm. The catalytic results showed that the choice of stabilizer, the stabilizer to Au weight ratio, thermal treatment of the catalyst, affect catalytic activity and selectivity/yield to the desired products. When PVA was the chosen stabilizer, the highest yield to furan-2-acrolein (33%) was attained with a PVA to Au weight ratio of 2.4. On the contrary, when PVP was the stabilizer, the best catalytic performance was achieved in its absence, with the yield of furan-2-acrolein reaching 21%. These results showed the strong impact of stabilizer to control catalytic activity and to enhance, in the case of PVA, the yield to the target product, whereas a strong negative effect was observed with PVP. Moreover, a mild thermal treatment of the catalyst and a washing step for the removal of the stabilizer from the catalyst had a positive effect on the catalytic performance.

1. Introduction

Furfural is one of the most important building block molecules derived from biomass, which can be utilised for the production of a high number of value-added chemicals [1-3]. After bioethanol, furfural is the second most obtained product in the sugar platform. Furfural can be produced industrially from xylose using acid catalysts, through a catalytic dehydration process with an annual production volume of more than 200000 tonnes [4,5]. Using furfural as platform molecule, a broad spectrum of chemical processes could be carried out, such as hydrogenation, oxidation, condensation, alkylation, decarbonylation, and ring-opening. From these processes, a large variety of important chemicals can be produced, such as, for example, phenol-furfural-resins, furfuryl alcohol, tetrahydrofurfuryl alcohol, furan, tetrahydrofuran, furoic acid, and other valuable products [6-11].

In this sense, furoic acid (FAc) can be employed for a number of applications, being considered as a suitable flavoring ingredient, in addition of its use as bactericide and fungicide [12]. Moreover, furoic acid has a potential in the field of optic technology [13]. Furoic acid is currently produced industrially via a Cannizzaro reaction with NaOH, with a yield of 50% (Scheme 1).
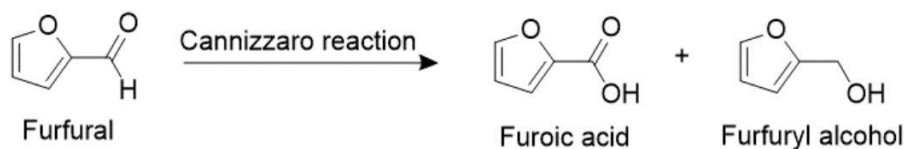
Scheme 1. Cannizzaro reaction for the furfural.

However, there is an interest to perform the oxidation of furfural to furoic acid using heterogeneous catalysts to improve the efficiency and the sustainability of this process at mild reaction conditions, instead of using strong oxidants, like chlorite, permanganate, or chromate, which have serious environmental effects [14,15].

In order to replace these strong oxidants, the use of noble metals has emerged as potential alternative in the presence of oxygen or hydrogen peroxide. Thus, it has been

shown that high selectivity to FAc (92%) can be achieved in the presence of an Ag$_2$O/CuO catalyst [16]. Another example is the use of supported Au-Pd bimetallic nanoparticles, where AuPd/MgO catalysts have been tested for the selective oxidation of furfural to furoic acid, evaluating several reaction parameters, such as the effect of base (NaOH) and molecular oxygen, which could influence the activity. It was reported that a furfural conversion of 88% with a high FAc yield of 84% could be attained [17].

In the last decade, cascade reactions with furfural have been investigated, in the presence of alcohol and water as the desired solvents. The reported cascade reactions (Scheme 2) could be either an oxidative esterification, leading to the formation of alkyl furoates, that can be used to produce flavors and fragrances, as well as in the fine chemical industry, or oxidative condensation to furan-2-acrolein derivatives that can be utilized for the preparation of high-quality aviation kerosene [18].

Several parameters can influence the selectivity on the route followed in the oxidation process. Thus, the chain length is one of the parameters that affect: short-chain alcohols help the formation of oxidative condensation products, while alcohols with longer chains increase the esterification selectivity. It has been pointed out that the selectivity towards oxidative condensation follows the next trend: ethanol = n-propanol > i-propanol > n-butanol > n-hexanol [19]. In addition, the nature of the support should be considered: weak acid sites favor condensation products, thus support's acidity is favorable if this route is preferred. Besides, the promoting effect of the base is another important parameter influencing selectivity. It has been established that an increase in basicity also favors the formation of oxidative condensation products. However, this basicity must be carefully tuned, since too strong bases can cause uncontrolled polymerization.

In the case of the oxidative esterification of furfural, the catalytic performance of supported Au nanoparticles and the role of support and Au particle size have been investigated. For example, Manzoli et al. have carried out a systematic study of the catalytic performance of Au nanoparticles supported on ZrO$_2$, TiO$_2$ and CeO$_2$ [20]. The comparison between the Au-based catalysts prepared by sol-immobilization method showed that using ZrO$_2$ as support a better catalytic performance was achieved in terms of conversion and selectivity. These authors propose the enhanced catalytic performance

3

as due to improved Au NPs dispersion and the presence of free OH groups on the catalyst surface, which facilitates the formation of hydrogen-carbonate species and, therefore, increasing the catalytic activity. In this way, it was explained why Au/CeO_2 showed worst catalytic performance than Au/ZrO_2, as well as the high selectivity of Au/TiO_2. Centi et al. demonstrated as well, the effectiveness of ZrO_2 as support for Au NPs for the oxidative esterification reaction, from the screening of a high number of synthesized and commercial catalysts [21].

Because of the importance of the presence of OH groups on the surface of the support, Ferraz et al. reported the use of MgO, as support, and methanol as the chosen alcohol [22]. In particular, they have synthesized supported Au nanoparticles via sol-immobilization method, using different oxides as supports, such as MgO, CaO, SrO and BaO. Au/MgO showed 95% methyl furoate (MF) yield, with a high catalytic performance and good stability after reusability. Moreover, a range of alcohols were tested, such as ethanol, isopropanol, n-butanol, and isopentanol, leading to the formation of the corresponding esters (ethyl-, isopropyl-, n-butyl, and isopentyl furoates) with high selectivity (>99%). Linear and branched esters were formed, but the long-chain linear alcohols resulted in higher yields, such as n-butyl furoate in 94% yield.

In the case of furfural condensation, the chosen alcohol in most of the reported studies is ethanol, since the desired product of the oxidative condensation is the furan-2-acrolein (Fur2Acr), which could find application as intermediate for the synthesis of drugs and fragrances. Pt and Au are the most common metals used for this reaction. For example, Liu et al. have synthesized Pt NPs supported on FeO_x–hydroxyapatite (FH), hydroxyapatite (H), hydrotalcite (HT), Fe_3O_4, Al_2O_3 and ZrO_2 [23]. It was demonstrated that Al_2O_3, FH and H favor the formation of smaller Au nanoparticles, with a mean Au nanoparticle size between 5 and 8 nm, as deduced by TEM analysis, quite different from 12 nm for HT and 26 nm for ZrO_2. Higher conversion and selectivity over 65% to furan-2-acrolein were attained with Pt/HT and Pt/Al_2O_3 catalysts. The authors concluded that the simultaneous presence of small-medium sized Au nanoparticles, as well as weak acid sites could promote reactivity. This research group also showed the efficiency of Au-based catalysts, by testing a wide range of catalysts (Au/Al_2O_3, Au/HTc, Au/CeO_2, Au/Fe_3O_4, Au/Nb_2O_5) prepared by deposition-precipitation method. The catalytic results

showed that the optimum catalytic performance was obtained by using Al_2O_3 as support [24].

Recently, Tong et al. have shown the highly efficient oxidative condensation of furfural with ethanol, in the presence of Au/CaO catalysts and ethanol as solvent [25]. They reported a 86% conversion with 82% selectivity to Fur2Acr, demonstrating, by elucidating the reaction mechanism, the synergistic effect between Au nanoparticles and basic CaO support.

The reaction mechanism of the oxidative condensation was described by Tong et al. [24]. In the first step, ethanol is oxidized to acetaldehyde (Scheme 2). The presence of a base such as Na_2CO_3 favors the extraction of a H^- in the alpha position of the carbonyl group of acetaldehyde, leading to the formation of an enolate. Then, this enolate can condensate with the carbonyl group of FUR. At the same time, the obtained enolate can also interact with other acetaldehyde molecules. The amount of the base, as well as its strength, must be modulated, since weak bases hardly promote the oxidative condensation, whereas strong ones give rise to uncontrolled condensation processes.

On the other hand, the oxidative esterification reaction to yield ethyl furoate must take place through the formation of the hemiacetal, since furoic acid was not detected in any case. Furthermore, it has been reported in the literature that furfural can react with alcohols at relatively mild temperatures, obtaining their respective acetals and hemiacetals [26].

Supported gold catalysts have also shown high catalytic performance in terms of activity, stability, and selectivity, for a range of organic reactions [27–30]. For example, gold catalysts have shown promising results for the oxidation of CO at low reaction temperature [31]. Moreover, in the presence of H_2, H_2O and CO_2, gold catalysts can be efficiently used for applications regarding fuel cells [32,33]. Efficient gold catalysts have been developed for the selective oxidation and epoxidation of alkenes [34-36] and alcohols [37-39] and for the selective hydrogenation of unsaturated carbonyl compounds and nitro groups [40,41.] Particularly, effective gold catalysts were developed for alcohol, polyol, and glucose oxidation in the presence of base for the first time by Rossi and Prati [42-45], and, afterwards, many research groups showed by following studies the effectiveness of supported Au nanoparticles for fine chemical synthesis [46-48].

In this paper, a series of supported gold nanoparticles has been prepared by using a colloidal method for studying the influence of several parameters for the oxidative condensation of furfural to furan-2-acrolein. Especially, in this work, it is reported the influence on the catalytic activity of experimental parameters such as the nature of the stabiliser, amount of stabiliser used (stabilizer to Au weight ratio), thermal and washing treatments for the removal of stabiliser and, finally, reaction temperature. The impact of stabiliser has been extensively studied for a range of reactions and the importance on controlling, not only the morphological properties of the supported nanoparticle, but also the influence in controlling the activity, selectivity and stability on a range of catalytic reactions [49-63]. Two different stabilisers were used: poly(vinyl alcohol) (PVA) and poly(vinyl pyrrolidone) (PVP). The catalysts were characterized before and after catalytic testing using a range of characterisation techniques.
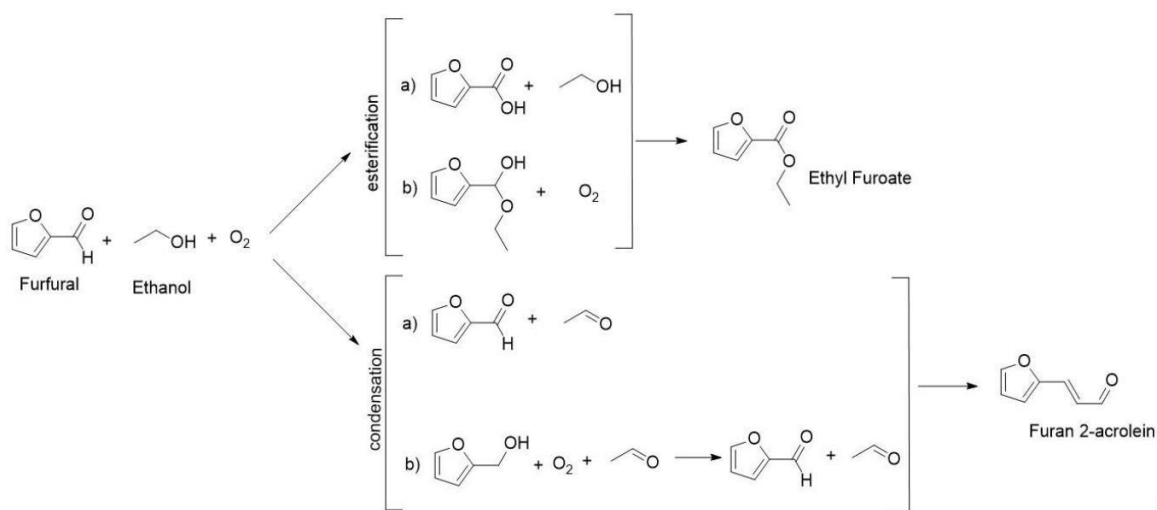
Scheme 2. Reaction pathway for furfural oxidative condensation and oxidative esterification.

2. Materials and Methods

2.1. *Materials*

The supported Au catalysts were prepared by using a colloidal method [63]. Tetra chloroauric(III) acid (Sigma Aldrich, 99.99 %), poly(vinyl alcohol) (PVA, Sigma Aldrich, MW 13 000–23 000 g mol^{-1}, hydrolysed 87–89 %), poly(vinyl pyrrolidone) (PVP, Sigma Aldrich, MW 29000 g mol^{-1}), poly(ethylene glycol) (PEG, Sigma Aldrich,

MW 8000 g mol^{-1}), sodium borohydride (Sigma Aldrich, powder, ≥98.0%) and activated carbon SX1G (AC, Norit) were used for catalyst preparation.

The catalysts prepared have been tested in the furfural esterification using ethanol (VWR, 96%), Na$_2$CO$_3$ anhydrous (VWR, 100 %), furfural (Sigma Aldrich,99%). O-xylene has been used as internal standard (Aldrich, 99.9%). For the calibration curves, it was used 3-(2-furyl)acrolein (furan-2-acrolein, Fur2Acr) (Sigma Aldrich, 99%) and ethyl-2-furoate (Sigma Aldrich, 99%).

2.2. Catalyst preparation

A typical preparation protocol is described below for the preparation of 1 g of catalyst: 0.0209 g of HAuCl$_4$ x 3H$_2$O were dissolved in 390 ml of distilled water (53.58 mg/L of gold precursor – 1.30 x 10^{-4} M Au). Then, the desired volume of stabiliser (PVA) or (PVP) solution (0.1010 g/ml) was added. After 3 minutes, 0.0096 g of sodium borohydride dissolved in 2.5 ml of water was added to the solution under stirring (NaBH$_4$:Au molar ratio= 5:1) to obtain a red colloidal dispersion. The Au colloidal solution was stirred for a period of 30 minutes and 0.99 g of support (activated carbon) was added to the solution to immobilize the gold preformed colloidal nanoparticles to obtain 1 wt.% of nominal Au loading. The pH of the solution was adjusted until pH=2 by the addition of concentrated sulfuric acid. The slurry solution was stirred at room temperature for 1 h. Then, the catalyst was filtered using a Buchner funnel. The catalyst was washed several times with distilled water until the filtrated aqueous solution reached pH of 7. Finally, the catalyst was firstly dried overnight at room temperature conditions and afterwards it was dried at 80 °C in an oven for 4 h in static air conditions. Catalysts were prepared by varying the type (PVA or PVP) and the amount of stabilizing agent (stabilizer:Au weight ratio 0, 0.3, 0.6, 1.2 and 2.4) as previously we have reported [63,64].

For the thermally treated catalyst, the following experimental protocol was followed: the catalyst was heated in a continuous flow reactor in air (flow rate= 20 ml/min), with a heating ramp of 5 °C/min from room temperature to the desired temperature (120, 200 or 250 °C) followed by an isotherm step of 2 h in air. After that, the atmosphere was switched to N$_2$ (flow rate= 20ml/min), maintaining the same reaction temperature for 30

minutes, and, then, another isothermal step at the same temperature was kept for 1 h in the presence of H_2 with a flow of 20 ml/min. Finally, the catalyst was cooled down at room temperature under the flow of H_2. The heat treatment at various temperatures was carried out on Au/AC PVA catalysts with PVA:Au weight ratio 0.6.

For the catalyst with a washing treatment, the following experimental protocol was followed: the catalyst was mixed with 20 ml of distilled water and a slurry solution was formed. The slurry solution was kept at 60 °C for 4 h under stirring. Then, the catalyst was again filtered, as previously, and dried at room temperature overnight. Finally, the solid was dried in the oven at 80 °C for 4 h.

2.3. Characterization of catalysts

The characterisation of the catalysts using UV-Vis, XRD and TEM techniques was reported in our previous work [63,64].

Transmission electron microscopy (TEM) images were obtained using a TEM/STEM FEI TECNAI F20 microscope at 200 keV and a TEM Talos F200X instrument. Samples were suspended in ethanol and treated by ultrasound for 15 min. A drop of the suspension was deposited on "quantifoil-carbon film" supported by a grid of Cu and dried before analysis.TEM images were processed by using the Digital Micrograph Software by Gatan Inc." and ImageJ to process TEM images and IA Imaging and Analysis Offline by FEI company for STEM-HAADF images in order to determine average particle size and particle size distribution. More than 400 NPs were measured, coming from different sites of interest, for each sample. X-ray photoelectron spectroscopy (XPS) spectra were recorded on a Physical Electronic spectrometer (PHI Versa Probe II) using monochromatic Al K radiation (52.8 W, 15 kV, 1486.6 eV) and a dual-beam charge neutralizer for analyzing the core-level signals of the elements of interest with a hemispherical multichannel detector. The XPS spectra of the samples were recorded with a constant pass energy value at 29.35 eV and a beam diameter of 100 µm. The energy scale was calibrated using Cu $2p_{3/2}$, Ag $3d_{5/2}$, and Au $4f_{7/2}$ photoelectron lines at 932.7, 368.2, and 83.95 eV, respectively. The X-ray photoelectron spectra obtained were analysed using PHI SmartSoft software and processed using the MultiPak 9.6.0.15 package. The binding energy values were referenced to C 1s signal at 284.5 eV. Shirley-

type background and Gauss–Lorentz curves were used to determine the binding energies. Atomic concentration percentages of the characteristic elements were determined considering the corresponding area sensitivity factor for the different measured spectral regions.

2.4. Catalytic test

The catalytic tests were carried out in a batch reactor (total volume: 10 mL), consisting of a stainless-steel autoclave with a Teflon cup inside, and the reaction conditions used have been previously reported [65,66]. A blank test was performed, in the absence of catalysts, and no furfural conversion was detected, thus demonstrating that the Teflon cup is inert.

Briefly the following experimental procedure was carried out: 6 mL of a mixture of ethanol and O-xylene (internal standard, ethanol:o-xylene volume ratio of 1:0.0067) was added in the reactor with 25 mg of catalyst, 0.1 g of base (Na_2CO_3), and 86 µL of furfural. Then, the reactor was closed and was firstly purged with N_2 and then filled with molecular oxygen at a total pressure of 0.6 MPa. Then, the reactor was placed on a magnetic hot plate stirrer to heat and maintain the reactor at the desired reaction temperature, e.g., 120 °C and a stirring rate of 350 rpm. After 6 h of reaction, the vessel was removed from the hot plate, the reactor was cooled down at room temperature and the liquid was separated from the catalyst by filtration. The liquid phase was analyzed through gas chromatography, using a TBR-14 column, and a FID detector.

The solid instead was washed with water to remove the sodium carbonate in excess.

The quantification of the compounds and the calculation of conversion and yield was carried out through the determination of the response factor for each chemical compound and using o-xylene as the internal standard.

3. Results and discussion

3.1. Characterization of the catalysts

The synthesized catalysts (Au-PVA, Au-PVP) have been characterized thoroughly in our previous work [63,64], using a range of characterization techniques, such as, UV-Vis spectroscopy, XRD, TEM and XPS and the data have been included as part in the supplementary information (Tables S1-S5, Figures S1-S7). In the present work, it is

reported new characterization of the spent catalysts for the studied reaction and the effect of thermal and washing treatments for specific catalysts. In the following paragraph a summary and brief description of the main characterization data is presented.

TEM analysis for the Au/AC-PVA catalysts showed that increasing the PVA amount the mean Au particle size (Table 1) was reduced from 8 to 2 nm and a narrower particle size distribution was observed. In the absence of PVA, larger and agglomerated Au nanoparticles were evident, pointing out a poor dispersion of Au nanoparticles on the support surface. The incorporation of PVA exerts a positive effect, since smaller Au nanoparticles and a better Au dispersion were achieved. When PVP was chosen as stabilizer, only when the PVP/Au weight ratio was in the range of 0.3-0.6 the mean gold particle size was relatively small, with mean value of 5.5 nm. Instead, in the absence of PVP and when a high PVP/Au weight ratio (above 0.6) was used, an increase of the mean Au particle size was observed. These results indicate that not only the amount of the stabilizer, but as well the choice and the nature of the stabilizer influence on the mean Au particle size and the dispersion of the Au nanoparticles onto the support.

Table 1. Mean particle size for supported Au nanoparticles using PVA and PVP with different polymer to Au weight ratio, as determined by TEM analysis [63,64].

Samples	Stabilizing polymer	Stabilizer:Au weight ratio	Mean particle size of Au (nm)
Au/AC PVA0	None	0	7.9 ± 6.3
Au/AC PVA0.3		0.3	4.3 ± 3.6
Au/AC PVA0.6	PVA	0.6	2.7 ± 1.6
Au/AC PVA1.2		1.2	2.6 ± 2.1
Au/AC PVA2.4		2.4	2.4 ± 1.2
Au/AC no HT			2.7 ± 1.6
Au/AC HT120	PVA	0.6	4.2 ± 2.3
Au/AC HT200			4.9 ± 2.9
Au/AC HT250			5.8 ± 4.1
Au/AC PVP0.3		0.3	5.5 ± 3.6
Au/AC PVP0.65	PVP	0.65	5.6 ± 3.9
Au/AC PVP1.2		1.2	7.4 ± 4.7
Au/AC PVP2.4		2.4	8.4 ± 4.9

Concerning the XPS analysis of the whole series of the Au/AC catalysts, metallic Au species without a significant change in the Au $4f_{7/2}$ binding energy (B.E. values were in the range of 84.0-84.1 eV) were detected (Supplementary Information, Table S3). Moreover, the surface composition was analyzed, focusing on the surface Au/C atomic ratio. Increasing the PVA/Au weight ratio from 0 to 0.3, an initial increase in the surface Au/C atomic ratio was observed from 0.028 to 0.039, whereas a further increase of the PVA/Au weight ratio from 0.3 to 2.4 led to a decrease in the Au/C surface atomic ratio from 0.039 to 0.022. This observed trend could be explained by the decrease of mean gold particle size, which causes an initial increase in the Au/C surface atomic ratio. However, at a higher amount of PVA, the surface of gold nanoparticles could be substantially covered by the presence of PVA, causing a decrease in the Au/C surface atomic ratio. In the case of the Au/AC-PVP catalysts, an increase in the PVP/Au weight ratio from 0 to 2.4 diminishes the Au/C surface atomic ratio from 0.028 to 0.0013.

3.2. Catalytic activity

3.2.1. Furfural oxidation: Effect of the reaction time

Furfural (FUR) is an important furan compound that could be used as building block derived from lignocellulosic biomass with a very high potential for biorefineries development. A range of different reactions could be studied using furfural as starting reagent, but, in this work, the attention has been focused on the oxidation reaction, especially on the oxidative condensation. Moreover, it must be taken into account that the amount of catalyst used in the present work, 25 mg, is lower than that used in other papers dealing with similar processes, in such as way that the comparison of different catalysts can be carried out.

Initially, as a reference catalyst to evaluate the effect of reaction time, and eventually the formation of intermediates and products to unveil the reaction pathways, a Au/AC catalyst was used (Figure 1).
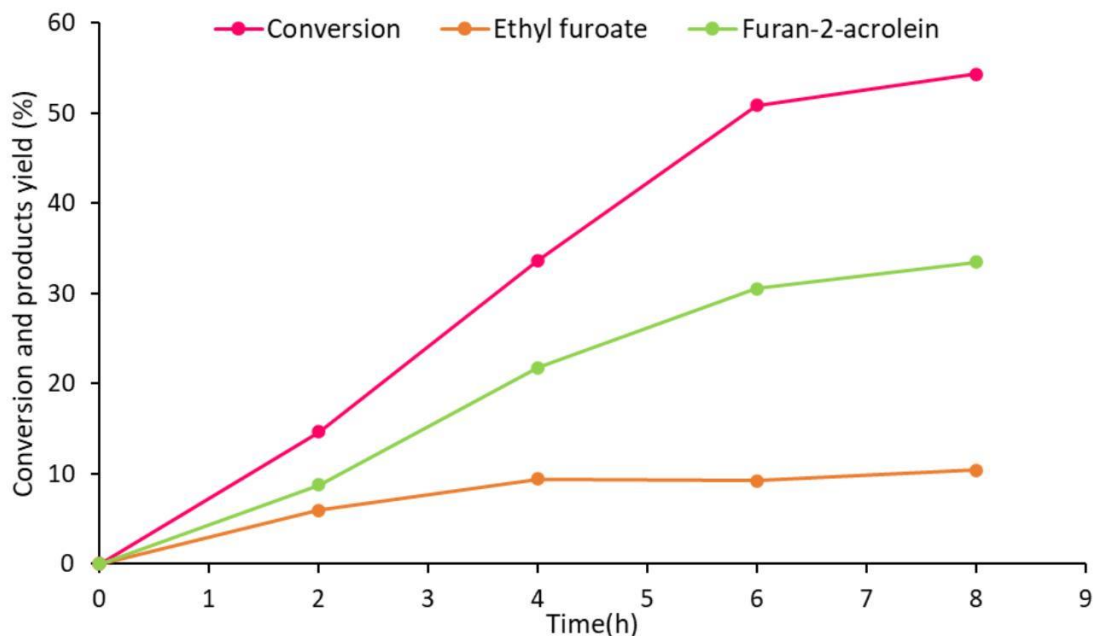
Figure 1. Conversion and product yields as a function of reaction time. (Experimental conditions: furfural= 86 µL, ethanol= 6 mL, 0.025 g of Au/AC PVA2.4, 0.1 g Na_2CO_3, 0.6 MPa O_2, T= 120 °C, stirring rate= 350 rpm).

Figure 1 shows the catalytic data obtained as a function of reaction time. At zero time (it is considered when the set point temperature was reached), no furfural (FUR) conversion and product yield were detected. After 2 h of reaction time, the FUR conversion was only 14%, pointing out a very slow reaction rate, then a linearly increase to 34% and 51%, from 4 to 6 h of reaction, was observed. After 8 h, the conversion slightly increased, but reaching only 54%. The ethyl furoate (EtFur) yield did not change drastically as a function of reaction time: from a yield of 6% after 2 h to 9-10% after 4 h. The furan-2-acrolein (Fur2Acr) showed a similar trend to the conversion, raising from 8% after 2 h to 22% and 30% after 4 and 6 h, respectively, reaching a maximum value of 33% after 8 h of reaction time. Therefore, it could be seen that increasing the reaction time from 6 to 8 h did not greatly improve either the conversion or the yield of the products. Moreover, the difference between FUR conversion and yield sum from 4 to 6 h increased from 2% to 10%. Furthermore, as the reaction time increased from 6 to 8 h, a decrease in carbon balance was observed, that could be related to the fact that chemical species start to be irreversibly adsorbed on the catalyst surface, blocking active sites.

12

From the GC analysis, no other chemical species were detected. Tong et al. has previously showed that the increase in reaction time can lead to an increase in the number of secondary products, as a consequence of uncontrolled polymerization of FUR or Fur2Acr [24]. Moreover, GC-MS analysis has allowed to verify this possibility [66]. For all these reasons, the following catalytic tests were performed at 6 h.

3.2.2. Furfural oxidation: Screening of the catalysts

The next step of investigation was focused on the catalytic screening of the Au/AC PVA series, being reported in Figure 2 the influence of PVA to Au weight ratio used (0-2.4) on the catalytic performance, in terms of furfural (FUR) conversion and yields of ethyl furoate (EtFur) and furan 2-acrolein (Fur2Acr). It can be observed that the conversion of FUR did not change drastically, varying between 41% (Au/AC PVA0) and 51% (Au/AC PVA0.3). However, the yield trends for the two products were quite different. In particular, the EtFur yield increased with the PVA amount, reaching the maximum yield of 14% for the Au/AC PVA0.6. However, a higher PVA:Au weight ratio caused a yield decrease and, for Au/AC PVA2.4, a value of 10% was found. Regarding the Fur2Acr, the formation of smaller nanoparticles is facilitated by increasing the amount of PVA, as previously shown [64], thus promoting the formation of Fur2Acr, increasing from 17% for Au/AC PVA0 to 33% for Au/AC PVA2.4. The selectivity reported in Figure 3 also confirmed the trend already seen for the EtFur and Fur2Acr yields and it is clear that Au/AC PVA2.4 gave the higher selectivity for condensation products.
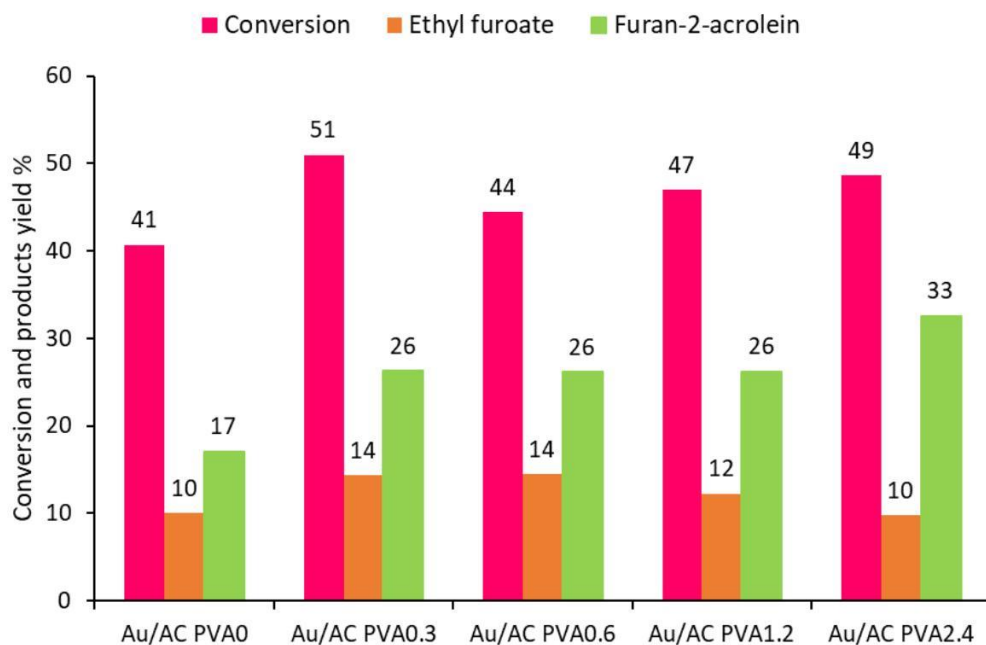
Figure 2. Conversion and yield of products as a function of PVA to Au weight ratio for Au/AC PVA catalysts. (Experimental conditions: furfural= 86 µL, ethanol= 6 mL, 0.025 g catalyst, 0.1 g Na_2CO_3, 0.6 MPa O_2, T= 120 °C, reaction time= 6 h, stirring rate= 350 rpm).
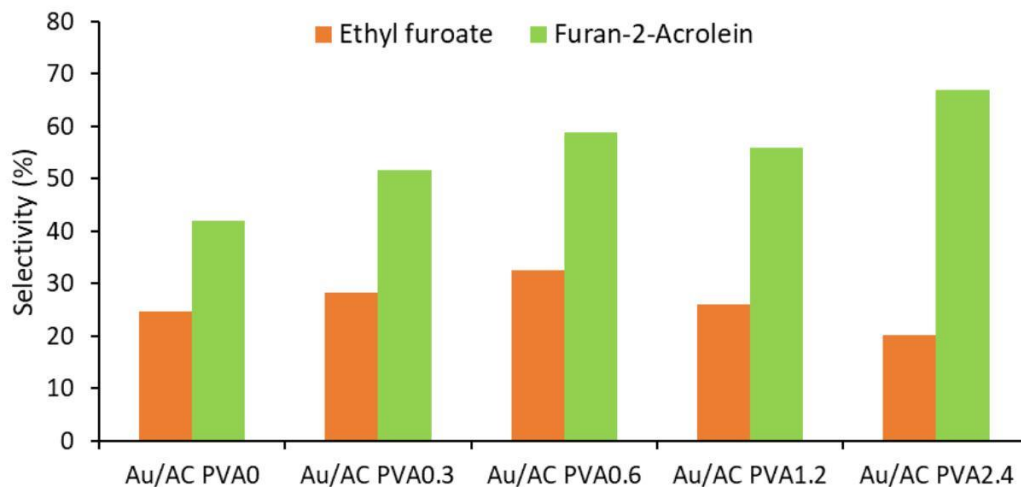
Figure 3. Selectivity to ethyl furoate and furan-2-acrolein as a function of PVA to Au weight ratio for Au/AC PVA catalysts. (Experimental conditions: furfural= 86 µL, ethanol= 6 mL, 0.025 g catalyst, 0.1 g Na_2CO_3, 0.6 MPa O_2, T= 120 °C, reaction time= 6 h, stirring rate= 350 rpm).

In order to elucidate the possible structure-activity relationship, the yield of the desired products as a function of Au mean particle size was plotted (Figure 4) and it illustrates how the dimension of the Au nanoparticles could influence the yield reported for the catalysts tested. The yield trends of the two main products are quite different. For the smaller Au nanoparticles (2.4 nm), ethyl furoate (EtFur) yield was very low, reaching 10%. A slight increase in the mean Au particle size led to an increase in the EtFur yield until reaching 14%, and the value remained constant for the catalysts with mean Au particle size of 2.7 nm and 4.3 nm. Then, additional increase in the mean Au particle size to 7.8 nm, followed by a decrease of EtFur to 10%. The furan-2-acrolein (Fur2Acr) yield instead decreases with the increase of the mean particle size of the Au nanoparticles: a yield of 33% was attained with the Au/AC PVA2.4 with the smaller Au nanoparticles (2.4 nm), and then the yield decreases to 17% for the sample with mean particle size of Au of 7.8 nm (Au/AC0). One hypothesis for the observed results is that the highest amount of PVA of the Au/AC PVA2.4 seems to provide a low yield of EtFur, whereas similar Au NP dimension (2.4 nm for Au/AC PVA2.4, 2.6 nm for Au/ACPVA1.2 and 2.7 nm for Au/AC PVA0.6), but at low PVA amount seems to increase the yield. At higher mean particle size (above ~5 nm), the yield to EtFur decreases again. Therefore, it is evident from these results that an optimum value of the PVA to Au weight ratio is needed as an optimum value of mean Au particle size.
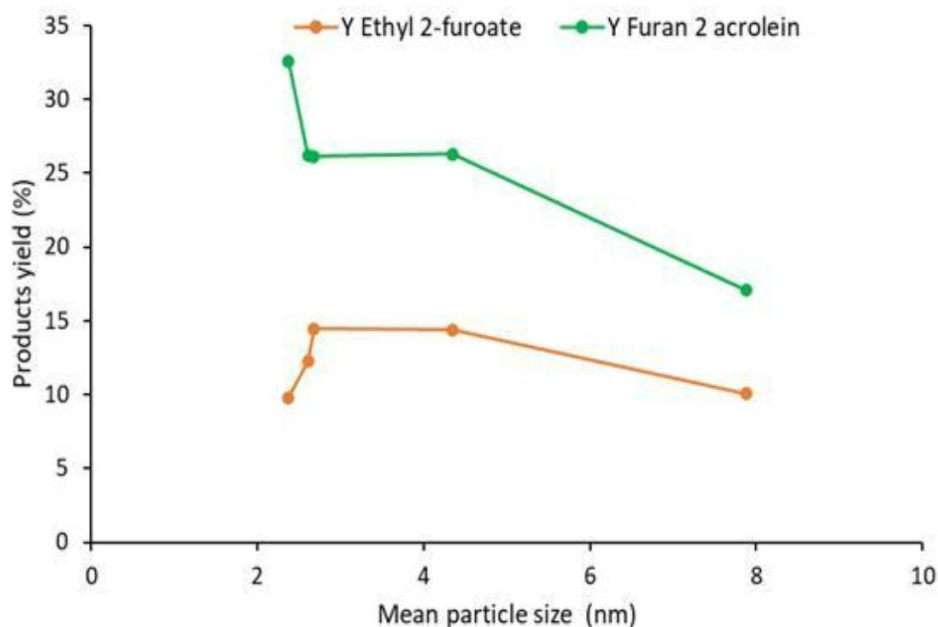
Figure 4. Yield of products as a function of mean Au particle size for Au/AC PVA catalysts (Experimental conditions: furfural= 86 µL, ethanol= 6 mL, 0.025 g catalyst, 0.1 g Na_2CO_3, 0.6 MPa O_2, T= 120 °C, reaction time= 6 h, stirring rate= 350 rpm).

Moreover, the comparison between the yield of products and surface Au/C atomic ratio was carried out to evaluate the effect of Au surface coverage. In Figure 5, two different catalytic trends could be observed. The ethyl furoate yield showed an increase with the surface Au/C atomic ratio. Instead, the Fur2Acr has a completely different trend as a function of the Au surface coverage. Au/AC PVA2.4 catalyst, with the lowest surface Au/C atomic ratio (0.022), gave the highest Fur2Acr yield; the following catalyst for surface Au/C atomic ratio (Au/AC PVA0) instead gives the lower yield (17%). A higher surface Au/C atomic ratio gives rise to yields between these two extreme values.
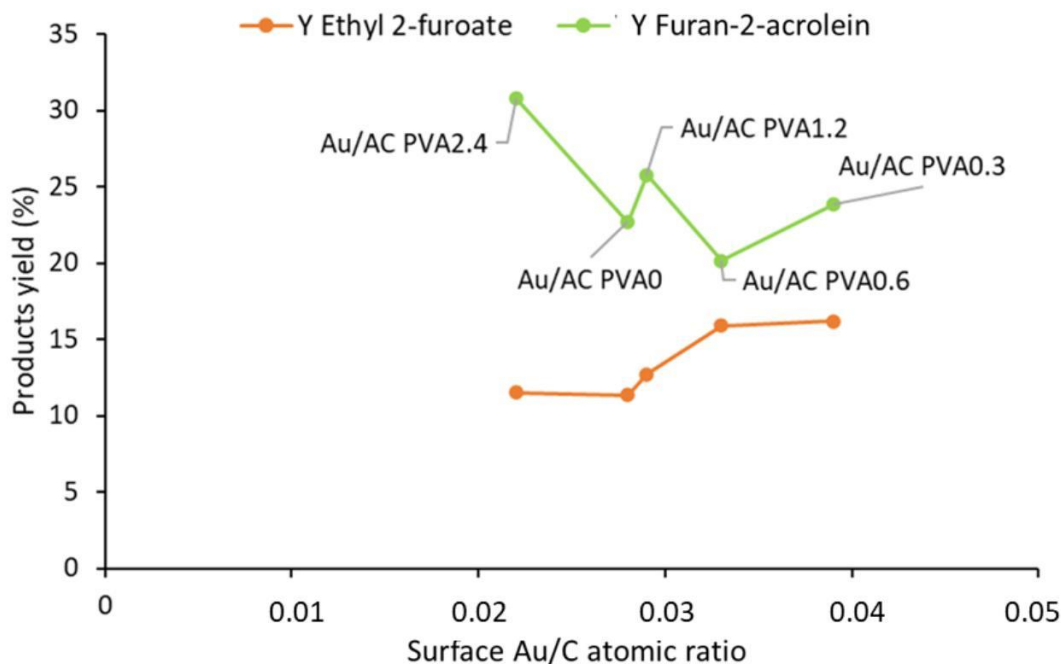
Figure 5. Yield of products as a function of surface Au/C atomic ratio for Au/AC PVA catalysts. (Experimental conditions: furfural= 86 µL, ethanol= 6 mL, 0.025 g catalyst, 0.1 g Na_2CO_3, 0.6 MPa O_2, T= 120 °C, reaction time= 6 h, stirring rate= 350 rpm).

Another parameter studied was the effect of the thermal treatment and washing step, aiming at the partial removal of the stabilizer, on the catalytic performance, as it has been shown previously in many reported studies [50-55]. In particular, it was seen that mild treatment conditions, like the washing (Au/AC washing) or thermal treatment at 120 °C (Au/AC HT 120 °C), provided a higher conversion and product yields than with the samples treated at higher temperature.

From the results shown in Figure 6, it can be inferred that mild thermal treatment at 120 °C and washing with warm water were the most effective, since the synthesized catalysts based on these experimental procedures have shown the highest catalytic performance. A slight increase in furfural conversion was observed for the treated catalysts, for example, the Au/AC without treatment reached 45% conversion, whereas Au/AC HT120 °C and washed Au/AC reached 47 and 52%. respectively. In terms of

17

Fur2Acr yield, a slight increase from 20% for the untreated Au/AC to 24% for Au/AC HT120 °C and washed Au/AC was observed. The higher reaction temperature used (over 120 °C) in the thermal treatment has a clear negative effect on the conversion of furfural and especially on the yield of EtFur. In particular, the conversion was decreased from 45 to 33% for Au/AC HT 200 °C and 35% for Au/AC HT 250 °C. The yield of EtFur showed a slight decrease from 16 to 13 and 12% for Au/AC HT 200 °C and Au/AC HT 250 °C, respectively. In the case of the yield of Fur2Acr, the observed values were similar (18-20%).
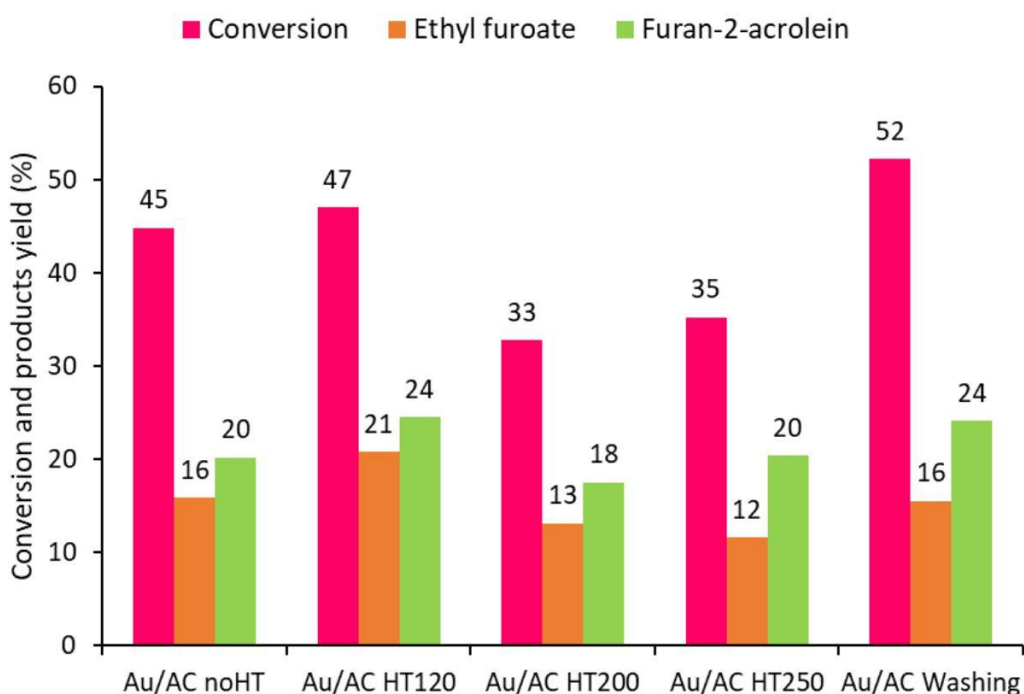
Figure 6. Conversion and yield of products as a function of heat and washing treatment protocol for Au/AC PVA catalysts with PVA:Au weight ratio 0.6. (Experimental conditions: furfural= 86 µL, ethanol= 6 mL, 0.025 g catalyst, 0.1 g Na_2CO_3, 0.6 MPa O_2, T= 120 °C, reaction time= 6 h, stirring rate= 350 rpm).

To explain the observed catalytic trend, the conversion of furfural and yield of products are plotted as a function of the surface Au/C atomic ratio, for the Au/AC without Au/AC no HT) and after thermal treatment (Au/AC HT120 °C, Au/AC HT200

°C and Au/AC HT250 °C), as illustrated in Figure 7. The mild conditions used for Au/AC HT120 °C permit to increase the number of active sites without a significant increase in the average Au particle size; in this way, the surface Au/C atomic ratio is higher (0.032) respect to the series of catalysts, and furfural conversion, EtFur and Furan-2-acrolein yields values also were the highest of the series. The increase in the average Au particle size for Au/AC HT200 (4.9 nm) and Au/AC HT250 (5.8 nm) decreases the surface Au/C atomic ratio (0.029 and 0.012, Tables S4, S5) and gives rise to a lower catalytic performance in terms of conversion and product yield.
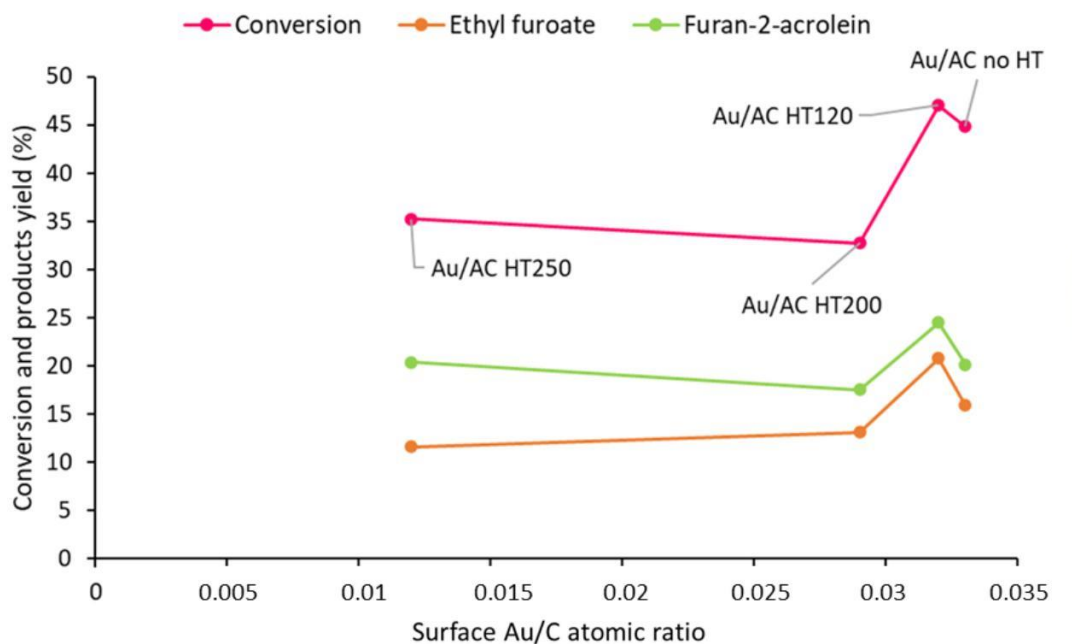
Figure 7. Yield of products as a function of surface Au/C atomic ratio for thermal treated and washed Au/AC PVA catalysts.

In the next step, the catalytic study of the Au/AC PVP catalysts was carried out for studying the influence and nature of stabiliser (PVA and PVP). As shown in Figure 8, the conversion of furfural was significantly decreased by increasing the amount of PVP. For Au/AC PVP0, the conversion was 50%, then conversion decreased to 10% for Au/AC PVP0.3 and to 8% for Au/AC PVP2.4. The same trend was observed for the products. The Ethyl-2-furoate has a 10% yield for the catalyst without polymer, but when the PVP is present, the yield decreased to 2% for Au/AC PVP0.3 and 1% for Au/AC PVP2.4. The

furan-2-acrolein yield was 21% in the absence of PVP, and then decreased to 4 and 2%, respectively. The trend from Figure 8 seems slightly fluctuating; this could be due to the low yield and conversion obtained, which could be affected more from the experimental error (the determination of deviation standard is reported in Table S6). However, it seems that an increase in the surface Au/C atomic ratio, that is accompanied with a decrease in particle size of Au and, simultaneously, the decrease in the stabilizing agent weight ratio, facilitates the catalytic activity for this series of catalysts in terms of conversion and yield. However, taking into account the surface coverage of Au, this trend changes after a specific PVP:Au weight ratio, and the trendlines reported in Figure 9 as a function of Au surface coverage appear like a volcano plot trend.
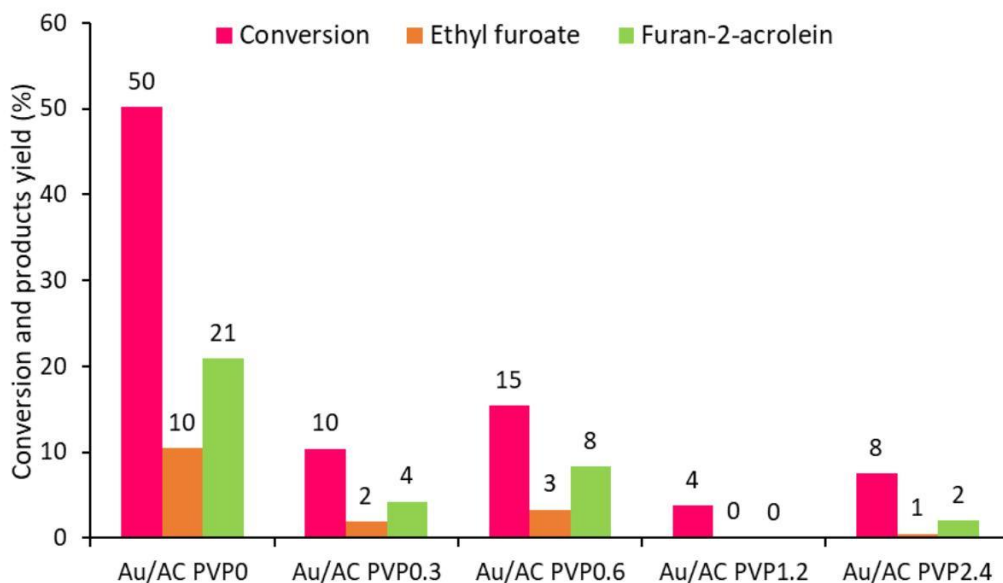
Figure 8. Conversion and yield to products as a function of PVP to Au weight ratio for Au/AC PVP catalysts. (Experimental conditions: furfural= 86 µL, ethanol= 6 mL, 0.025 g catalyst, 0.1 g Na_2CO_3, 0.6 MPa O_2, T= 120 °C, reaction time= 6 h, stirring rate= 350 rpm).
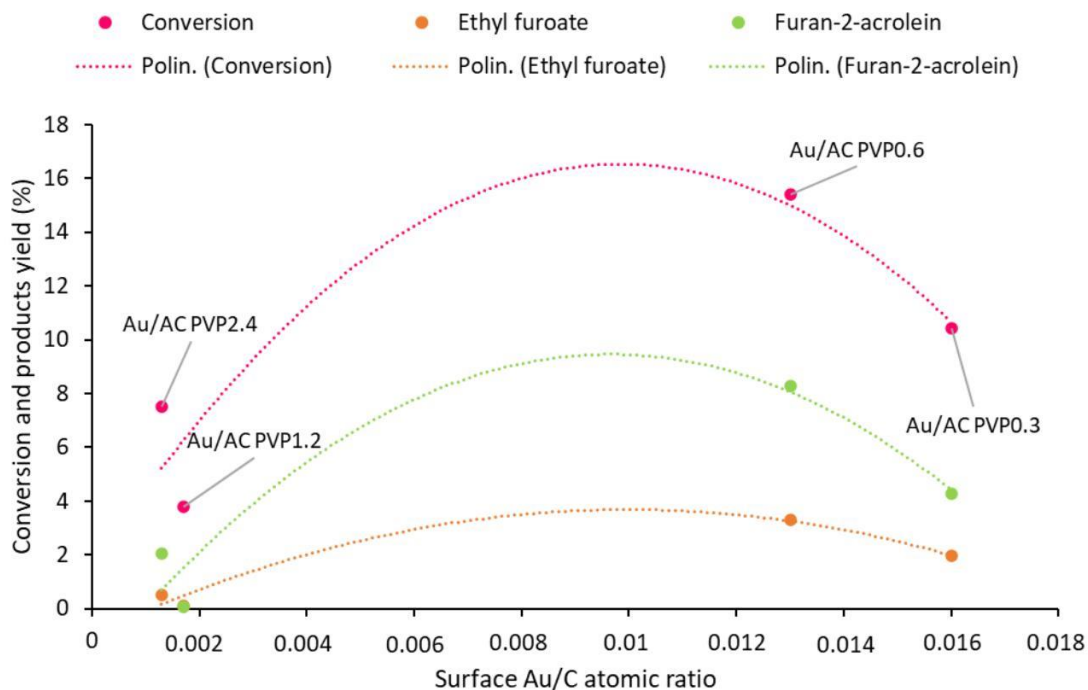
Figure 9. Yield of products as a function of surface atomic ratio Au/C for Au/AC PVP catalysts. (Experimental conditions: furfural= 86 µL, ethanol= 6 mL, 0.025 g catalyst, 0.1 g Na_2CO_3, 0.6 MPa O_2, T= 120 °C, reaction time= 6 h, stirring rate= 350 rpm).

3.2.3 Furfural oxidation: Effect of reaction temperature

The effect of reaction temperature on the oxidative condensation/esterification of furfural with ethanol was investigated to evaluate how this reaction parameter could influence the product selectivity and furfural conversion. To do that, it was decided to carry out tests at different temperatures (110-150 °C). However, a high temperature and long reaction time can affect the morphology of the supported Au nanoparticles. To study the morphology of the fresh and used catalysts (reaction conditions: T= 120 °C, 6 h of reaction time, stirring speed of 350 rpm), TEM analysis was performed of the fresh and used Au/AC PVA0, Au/ACPVA0.3, and Au/AC PVA2.4 catalysts (Figures S8-S10).

Table 2. Comparison between mean Au particle size by TEM analysis of fresh and spent Au/AC PVA catalysts.

Samples	Mean nanoparticle size of Au by TEM (nm)	
	- Fresh	Spent
Au/AC PVA0	7.9±6.3	14.0±6.4
Au/AC PVA0.3	4.3±3.6	6.1±3.0
Au/AC PVA2.4	2.3±1.2	5.5±2.6

The sample Au/AC PVA2.4 was chosen to investigate further the effect of the reaction temperature due to (i) the smallest mean particle size of Au, (ii) the best activity showed during the reaction and (iii) the good selectivity to Fur2Acr.

Figure 10 shows the Fur conversion and product yields as a function of reaction temperature. It can be seen that the increase in reaction temperature (from 110 °C to 150 °C) improves furfural conversion, starting from 35% at 110 °C until 90% at 150°C. In terms of product yields, the increase in reaction temperature seems not to affect drastically the yield of EtFur, which slightly decrease from 11 to 5%; in the case of Fur2Acr yield, the increase in reaction temperature improves the yield from 12% at 110 °C to 43% at 140 °C.

Figure 10. Conversion and yield of products as a function of reaction temperature. (Experimental conditions: furfural= 86 µL, ethanol= 6 mL, 0.025 g Au/AC PVA2.4, 0.1 g Na_2CO_3, 0.6 MPa O_2, T= 110-150 °C, reaction time= 6 h, stirring rate= 350 rpm).

The selectivity trend (Figure 11) reveals that 130 °C is the most suitable temperature to operate, having the best selectivity toward Fur2Acr (67%). Despite this good selectivity, the high temperature leads to a lower carbon balance, which reaches 50% at 150 °C. The worsening of the carbon balance could be due to the formation of polymerization products (the solution color darkens as shown in Figure S11 and it is observable a small peak at the GC for high retention time). Moreover, the presence of a small peak at low retention time observed from GC analysis is probably due to light products due to ethanol reactions, as Tong et al. have previously reported [23,24].

Figure 11. Selectivity to ethyl furoate and furan-2-acrolein as a function of reaction temperature. (Experimental conditions: furfural= 86 µL, ethanol= 6 mL, 0.025 g Au/AC PVA2.4, 0.1 g Na_2CO_3, 0.6 MPa O_2, T= 110-150 °C, reaction time= 6 h, stirring rate= 350 rpm).

It was already seen that Au/AC HT120 gives a slight improvement in catalytic performance for furfural reaction. To see if the increase in the temperature can modify the yield of the two products, the effect of the temperature was studied from 120 to 150 °C for Au/AC HT120.

A trend similar to that of Au/AC PVA2.4 was obtained. In particular, it could be seen that the increase in reaction temperature favors the conversion of furfural, which started from 45% at 120 °C and reached 82% at 150 °C (Figure 12). Moreover, a higher reaction temperature decreased the Etfur yield that dropped from 22 to 12% and increased the Furan-2-acrolein yield from 26 to 47%, in agreement with previous reports [64,65]. Finally, as shown in Figure 13, the Fur2acr selectivity was enhanced with the reaction temperature and 140 °C seems to be the optimum reaction temperature to obtain a higher oxidative condensation product yield. In addition, at 150 °C, a higher carbon loss was

observed (22% vs 10% at 140 °C), probably due to the formation of polymerization products.
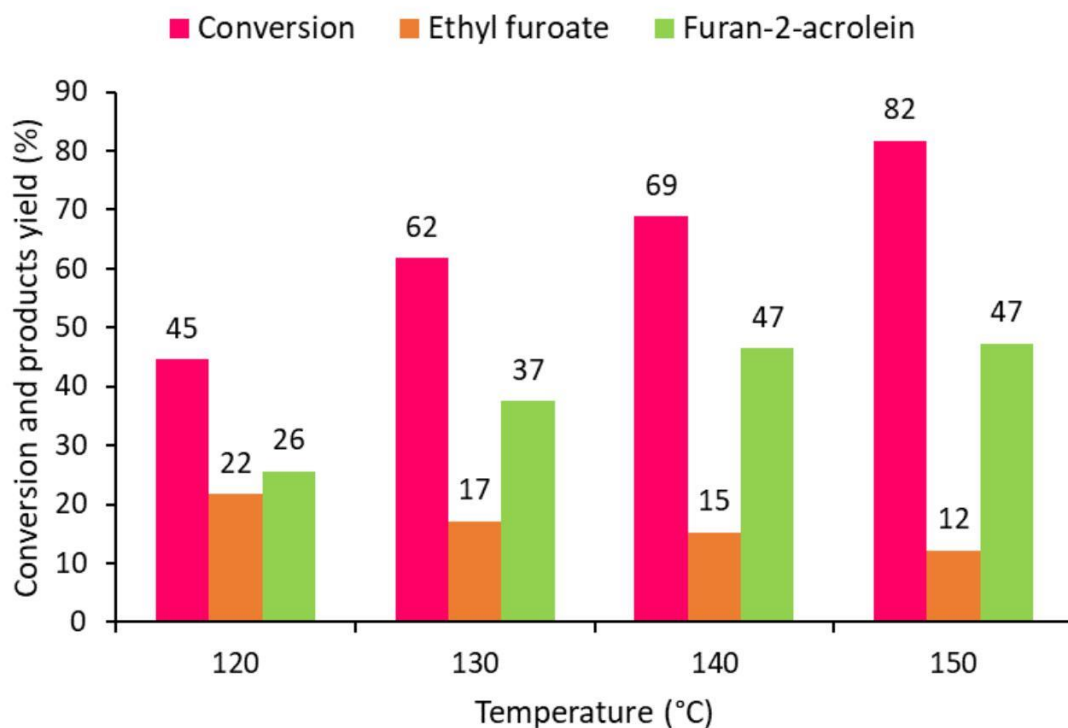
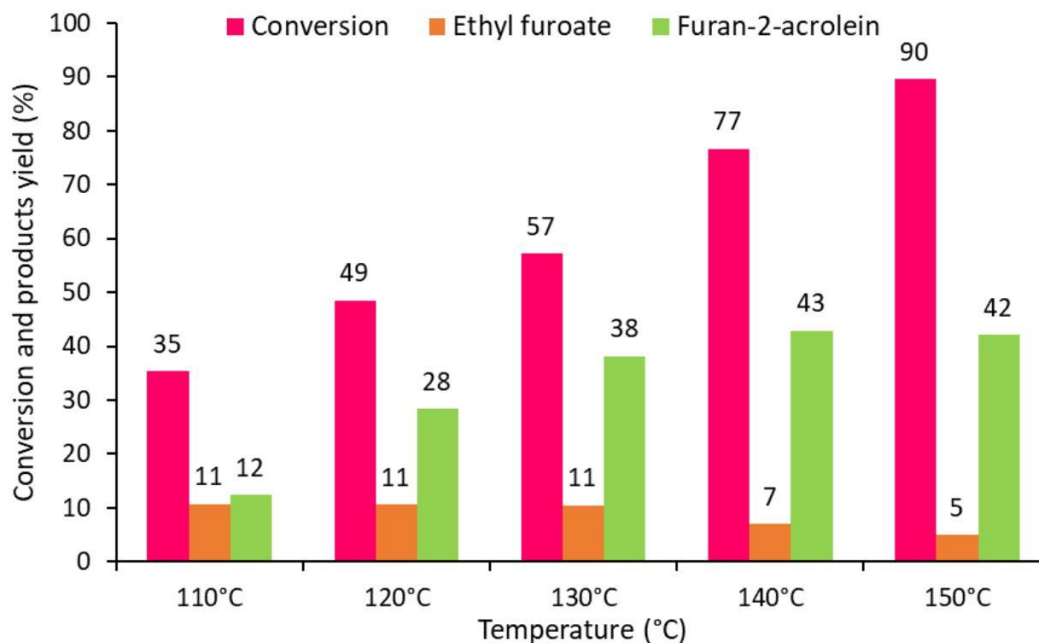**Figure 12.** Conversion and yield of products as a function of temperature. (Experimental conditions: furfural= 86 µL, ethanol= 6 mL, 0.025 g Au/AC HT120, 0.1 g Na_2CO_3, 0.6 MPa O_2, T= 120-150 °C, reaction time= 6 h, stirring rate= 350 rpm).
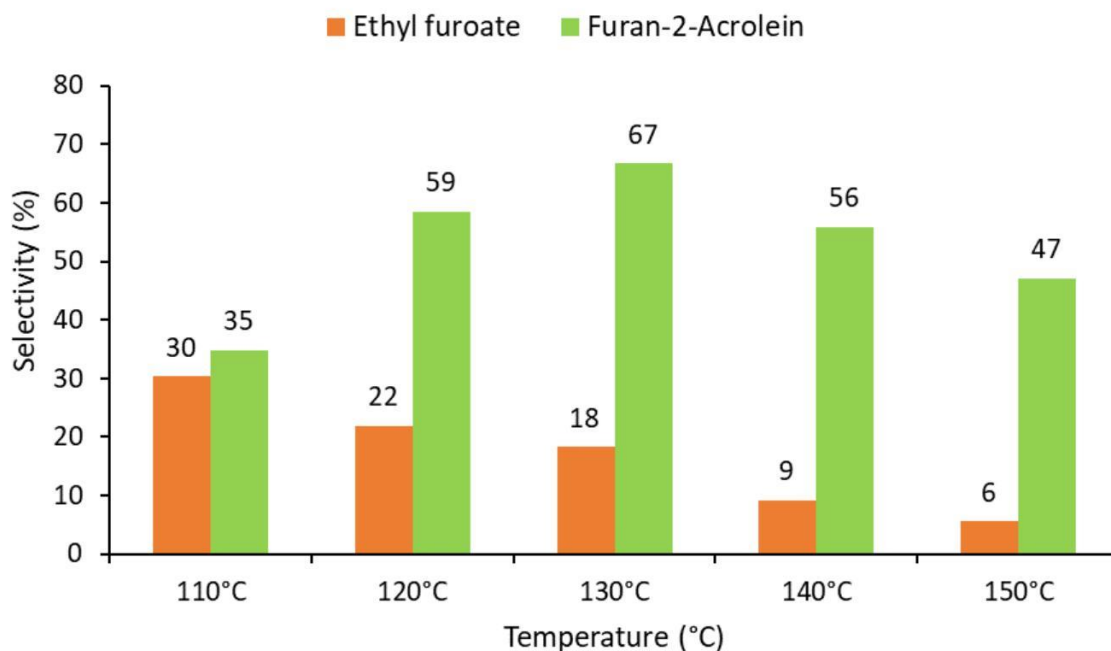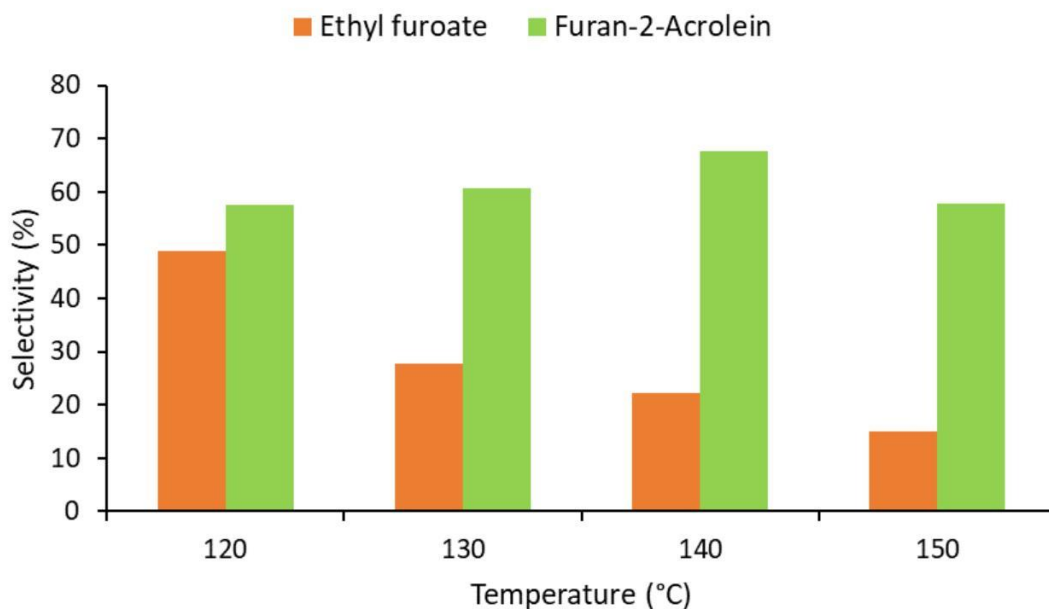
Figure 13. Selectivity to ethyl furoate and furan-2-acrolein as a function of reaction temperature. (Experimental conditions: furfural= 86 µL, ethanol= 6 mL, 0.025 g Au/AC HT120, 0.1 g Na_2CO_3, 0.6 MPa O_2, T= 120-150 °C, reaction time= 6 h, stirring rate= 350 rpm).

Finally, in the following table a comparison based on our previous catalytic studies is presented to show the effectiveness of the new catalytic systems with respect to the choice of metal, support and oxidant (Table 3). It is evident that Au-based catalysts showed a good yield with respect to Pd based catalysts at mild reaction conditions and using molecular oxygen as the chosen oxidant in the absence of H_2O_2 and lower mass of catalyst.

Table 3. Comparison of catalytic performance of Pd-based catalysts versus Au-based catalysts.

Samples	Pd-loading (wt.%)	Mass of catalyst (mg)	Temp. (ºC)	Reaction time (h)	Mass of Na_2CO_3 (mg)	Oxidant	Y_{F2A} (%)	Ref.
Pd-TiO$_2$	1	50	150	3	100	500 µL H_2O_2	60	[65]
Pd-beta	2	50	170	3	100	480 µL H_2O_2	39	[66]
Pd-Al$_2$O$_3$	2	50	170	3	100	480 µL H_2O_2	49	[66]
Pd-Fe$_2$O$_3$	2	50	170	3	100	480 µL H_2O_2	59	[66]
Pd-MgO	2	50	170	3	100	480 µL H_2O_2	70	[66]
Pd-SiO$_2$	2	50	170	3	100	480 µL H_2O_2	17	[66]
Au/AC PVA2.4	1	25	150	6	100	0.6 MPa O_2	47	This work

4. Conclusions

The catalytic performance of supported Au colloidal nanoparticles prepared by colloidal methodologies by varying the nature of stabilizer (PVA and PVP) and the effect of treatment of the catalyst (thermal or washing) was investigated for the oxidative condensation of furfural with ethanol. Depending on the stabilizer and the stabilizer/Au weight ratio, the mean gold particle size was varied in the range of 3-8 nm. The catalytic data showed that the choice and the amount of stabilizer had a significant impact on of catalytic activity, stability and selectivity to ethyl furoate and furan-2-acrolein. When the PVA to Au weight ratio was lower than 1.2, the optimal catalytic performance was obtained in terms of yield to furan-2-acrolein. In the case of PVP, the presence of PVP had a negative impact on furfural conversion and yields to the desired products. The difference in the catalytic performance was mainly attributed to the surface coverage of PVP on the active sites of the catalyst, due to the blocking of the active sites by the larger mean Au particle size. Regarding the thermal treatment, or washing step, for the removal of the stabilizer, a positive effect was found when a mild thermal treatment was applied.

In relation to the stability of the catalysts as a function of the PVA amount, it was found that, in the presence of the stabilizer (PVA), the mean Au particle size was diminished. Finally, the effect of reaction temperature was studied, and it was observed that a maximum yield to furan-2-acrolein was attained at 140 °C. These results demonstrate the role of stabilizer for tuning the size of Au nanoparticles and the strong influence of stabilizer to affect catalytic activity, yield to desired products and stability of the catalyst.

References

[1] C.H. Zhou, X. Xia, C.C. Li, D.S. Tong, J. Beltramini, Catalytic conversion of lignocellulosic biomass to fine chemicals and fuels. Chem. Soc. Rev. 40 (2011) 5588–5617.

[2] J.B. Binder, R.T. Raines, Simple chemical transformation of lignocellulosic biomass into furans for fuels and chemicals. J. Am. Chem. Soc. 131 (2009) 1979–1985.

[3] A. Corma, S. Iborra, A.Velty, Chemical routes for the transformation of biomass into chemicals. Chem. Rev. 107 (2007) 2411–2502.

[4] B. Kamm, PR. Gruber, M. Kamm, editors. Biorefineries—Industrial Processes and Products. Wiley-VCH, Weinheim; 2006

[5] I. Agirrezabal-Telleria, I. Gandarias, P.L. Arias, Heterogeneous Acid-Catalysts for the Production of Furan-Derived Compounds (Furfural and Hydroxymethylfurfural) from Renewable Carbohydrates: A Review. Catal. Today 234 (2014) 42−58.

[6] R. Mariscal, P. Maireles-Torres, M. Ojeda, I. Sádaba, M. López Granados, Furfural: A Renewable and Versatile Platform Molecule for the Synthesis of Chemicals and Fuels. Energy Environ. Sci. 9 (2016) 1144−1189.

[7] P.L. Arias, J. A. Cecilia, I. Gandarias, J. Iglesias, M. López Granados, R. Mariscal, G. Morales, R. Moreno-Tost, P. Maireles- Torres, Oxidation of Lignocellulosic Platform Molecules to Value- Added Chemicals Using Heterogeneous Catalytic Technologies. Catal. Sci. Technol. 10 (2020) 2721−2757.

[8] S. Campisi, D. Motta, I. Barlocco, R. Stones, T.W. Chamberlain, A. Chutia, N. Dimitratos, A. Villa. Furfural Adsorption and Hydrogenation at the Oxide-Metal Interface: Evidence of the Support Influence on the Selectivity of Iridium-Based Catalysts. Chemcatchem, 2022, *in press*.

[9] G.F. Tierney, S. Alijani, M. Panchal, D. Decarolis, M. Briceno de Gutierrez, K.M.H. Mohammed, J. Callison, E.K. Gibson, P.B.J. Thompson, P. Collier, N. Dimitratos, E. C. Corbos, F. Pelletier, A. Villa, P.P. Wells. Controlling the Production of Acid Catalyzed Products of Furfural Hydrogenation by Pd/TiO$_2$. ChemCatChem, 13 (2021) 5121-5133.

[10] S. Campisi, C.E. Chan-Thaw, L.E. Chinchilla, A. Chutia, G.A. Botton, K.M.H. Mohammed, N. Dimitratos, P.P. Wells, A. Villa, Dual-site-mediated hydrogenation catalysis on Pd/NiO: selective biomass transformation and maintenance of catalytic activity at low Pd loading. ACS Catalysis, 10 (2020) 5483-5492.

[11] S.M. Rogers, C.R.A. Catlow, C.E. Chan-Thaw, A. Chutia, N. Jian, R.E. Palmer, M. Perdjon, A. Thetford, N. Dimitratos, A. Villa, P.P. Wells. Tandem site-and size-controlled Pd nanoparticles for the directed hydrogenation of furfural. 7 (2017) 2266-227412.

[12] George Burdock, (1996). "P–Z indexes". Encyclopedia of Food and Color Additives. 3. Bob Stern. pp. 2359.

[13] B. Uma, S. Das, Jerome, S. Krishnan, B. Boaz, Milton, Growth, optical and thermal studies on organic nonlinear optical crystal: 2-Furoic acid. Physica B: Condensed Matter. 406 (2011) 2834–2839.

[14] E. Dalcanale, F. Montanari, Selective oxidation of aldehydes to carboxylic acids with sodium chlorite-hydrogen peroxide. J. Org. Chem. 51 (1986) 567–569.

[15] K.G. Sekar, Oxidation of furfural by imidazolium dichromate in acid medium. Int. J. Chem. Sci. 1(2003) 227–232.

[16] Q. Y. Tian, D. X. Shi and Y. W. Sha, A Convenient Synthesis of Amino Acid Methyl Esters. Molecules 13 (2008) 948–957.

[17] M. Douthwaite, X. Huang, S. Iqbal, P.J. Miedziak, G.L. Brett, S. Kondrat, J.K. Edwards, M. Sankar, D.W. Knight, D. Bethell, G.J. Hutchings, The controlled catalytic oxidation of furfural to furoic acid using AuPd/Mg(OH)$_2$. Catal. Sci. Technol. 7 (2017) 5284–529318.

[18] H. Li, A. Riisager, S. Saravanamurugan, A. Pandey, R.S. Sangwan, S. Yang, R. Luque, Carbon-increasing catalytic strategies for upgrading biomass into energy-intensive fuels and chemicals. ACS Catal. 8 (2017) 148-187.

[19] L. Yu, S. Liao, L. Ning, S. Xue, Z. Liu, X. Tong, ACS Sustainable Chem. Eng. 4 (2016) 1894–1898.

[20] M. Manzoli, F. Menegazzo, M. Signoretto, D. Marchese, Biomass Derived Chemicals: Furfural Oxidative Esterification to Methyl-2-furoate over Gold Catalysts. Catalysts 6 (2016) 107.

[21] C. Ampelli, G. Centi, C. Genovese, G. Papanikolaou, R. Pizzi, S. Perathoner, R.-J. van Putten, K.J.P. Schouten, A.C. Gluhoi, J.C. van der Waal, A Comparative Catalyst Evaluation for the Selective Oxidative Esterification of Furfural. Top. Catal. 59 (2016) 1659–1667.

[22] C.P. Ferraz, A.H. Braga, M.N. Ghazzal, M. Zielinski, M. Pietrowski, I. Itabaiana, J.F. Dumeignil, L.M. Rossi, R. Wojcieszak, Efficient Oxidative Esterification of Furfural Using Au Nanoparticles Supported on Group 2 Alkaline Earth Metal Oxides Catalysts. Catalysts 10 (2020) 43023.

[23] X. Tong, Z. Liu, L. Yu and Y. Li, A tunable process: catalytic transformation of renewable furfural with aliphatic alcohols in the presence of molecular oxygen. Chem. Commun. 51 (2015) 3674–3677.

[24] X. Tong, Z. Liu, J. Hu and S. Liao, Au-Catalyzed Oxidative Condensation of Renewable Furfural and Ethanol to Produce Furan-2-acrolein in the Presence of Molecular Oxygen . Appl. Catal. A 510 (2016) 196–203.

[25] Y. Gao, X. Tong, H. Zhang, A selective oxidative valorization of biomass-derived furfural and ethanol with the supported gold catalysts. Catal. Today 355 (2020) 238–245.

[26] J.M. Rubio-Caballero, S. Saravanamurugan, P. Maireles-Torres, A. Riisager, Acetalization of furfural with zeolites under benign reaction conditions. Catal. Today 234 (2014) 233-236.

[27] A.S.K. Hashmi, G.J. Hutchings, Gold Catalysis. Angew. Chem. Int. Ed. 45 (2006) 7896-7936.

[28] C.D. Pina, E. Falletta, L. Prati, M. Rossi, Selective oxidation using gold. Chem. Soc. Rev. 37 (2008) 2077-2095.

[29] A. Corma, H. Garcia, Supported gold nanoparticles as catalysts for organic reactions. Chem. Soc. Rev. 37 (2008) 2096-20126.

[30] A. Villa, N. Dimitratos, C.E. Chan-Thaw, C. Hammond, L. Prati, G.J. Hutchings, Glycerol oxidation using gold-containing catalysts. Acc. Chem. Res. 48 (2015) 1403-1412.

[31] M. Haruta, T. Kobayashi, H. Sano, N. Yamada, Novel Gold Catalysts for the Oxidation of Carbon Monoxide at a Temperature far Below 0 °C. Chem. Lett., 16 (1987) 405-408.

[32] P. Landon, J. Ferguson, B.E. Solsona, T. Garcia, A.F. Carley, A.A. Herzing, C.J. Kiely, S.E. Golunski, G.J. Hutchings, Selective oxidation of CO in the presence of H_2, H_2O and CO_2 via gold for use in fuel cells. Chem. Commun. (2005) 3385-3387.

[33] P. Landon, J. Ferguson, B.E. Solsona, T. Garcia, S. Al-Sayari, A.F. Carley, A. Herzing, C.J. Kiely, M. Makkee, J.A. Moulijn, A. Overweg, S.E. Golunski, G.J. Hutchings, Selective oxidation of CO in the presence of H_2, H_2O and CO_2 utilising Au/α-Fe_2O_3 catalysts for use in fuel cells. J. Mater. Chem., 16 (2006) 199-208.

[34] A.K. Sinha, S. Seelan, S. Tsubota, M. Haruta, A three-dimensional mesoporous titanosilicate support for gold nanoparticles: vapor-phase epoxidation of propene with high conversion. Angew. Chem. Int. Ed. 43 (2004) 1546-1548.

[35] M.D. Hughes, Y.-J. Xu, P. Jenkins, P. McMorn, P. Landon, D.I. Enache, A.F. Carley, G.A. Attard, G.J. Hutchings, F. King, E.H. Stitt, P. Johnston, K. Griffin, C.J. Kiely, Tunable gold catalysts for selective hydrocarbon oxidation under mild conditions. Nature 437 (2005) 1132-1135.

[36] S. Bawaked, N.F. Dummer, N. Dimitratos, D. Bethell, Q. He, C.J. Kiely, G.J. Hutchings, Solvent-free selective epoxidation of cyclooctene using supported gold catalysts. Green Chem. 11 (2009) 1037-1044.

[37] N. Dimitratos, J.A. Lopez-Sanchez, G.J. Hutchings, Selective liquid phase oxidation with supported metal nanoparticles. Chem. Sci. 3 (2012) 20-44.

[38] S. Campisi, M. Schiavoni, C.E. Chan-Thaw, A. Villa, Untangling the role of the capping agent in nanocatalysis: recent advances and perspectives. Catalysts 6 (2016) 185-205.

[39] A. Villa , M. Schiavoni, L. Prati, Material science for the support design: a powerful challenge for catalysis. Catal. Sci. Technol. 2 (2012) 673-682.

[40] M. Pan, A.J. Brush, Z.D. Pozun, H.C. Ham, W.-Y. Yu, G. Henkelman, G.S. Hwang, C.B. Mullins, Model studies of heterogeneous catalytic hydrogenation reactions with gold. Chem. Soc. Rev. 42 (2013) 5002-5013.

[41] A. Corma, P. Serna, Science, Chemoselective hydrogenation of nitro compounds with supported gold catalysts. 313 (2006) 332-334.

[42] L. Prati, M. Rossi, Gold on Carbon as a New Catalyst for Selective Liquid Phase Oxidation of Diols. J. Catal. 176 (1998) 552-560.

[43] F. Porta, L. Prati, M. Rossi, G. Scari, New Au(0) Sols as Precursors for Heterogeneous Liquid-Phase Oxidation Catalysts. J. Catal. 211 (2002) 464-469.

[44] F. Porta, L. Prati, Selective oxidation of glycerol to sodium glycerate with gold-on-carbon catalyst: an insight into reaction selectivity. J. Catal. 224 (2004) 397-403.

[45] M. Comotti, C.D. Pina, R. Matarrese, M. Rossi, The Catalytic Activity of "Naked" Gold Particles. Angew. Chem. Int. Ed. 43 (2004) 5812-5815.

[46] T. Ishida, N. Kinoshita, H. Okatsu, T. Akita,T. Takei, M. Haruta, Influence of the Support and the Size of Gold Clusters on Catalytic Activity for Glucose Oxidation. Angew. Chem. Int. Ed. 120 (2008) 9405-9408.

[47] C.D. Pina , E. Falletta, M. Rossi, Update on selective oxidation using gold. Chem. Soc. Rev. 41 (2012) 350-369.

[48] Y. Zhang, X. Cui, F. Shi, Y. Deng, Nano-Gold Catalysis in Fine Chemical Synthesis. Chem. Rev. 112 (2012) 2467–2505.

[49] K.Y. Lee, Y.W. Lee, J.H. Lee, S.W.Han, Effect of ligand structure on the catalytic activity of Au nanocrystals. Colloids and Surfaces A: Physicochem. Eng. Aspects 372 (2010) 146-150.

[50] C.J. Jia, F. Schüth, Colloidal metal nanoparticles as a component of designed catalyst. Phys. Chem. Chem. Phys. 13 (2011) 2457-2487.

[51] J.A. Lopez-Sanchez, N. Dimitratos, C. Hammond, G.L. Brett, L. Kesavan, S. White, P. Miedziak, R. Tiruvalam, R.L. Jenkins, A.F. Carley, D. Knight, C.J. Kiely, G.J. Hutchings, Facile removal of stabilizer-ligands from supported gold nanoparticles. Nat. Chem. 3 (2011) 551-556.

[52] R.C. Tiruvalam, J.C. Pritchard, N. Dimitratos, J.A. Lopez-Sanchez, J. K. Edwards, A. F. Carley, G.J. Hutchings, C.J. Kiely, Aberration corrected analytical electron microscopy studies of sol-immobilized Au+ Pd, Au {Pd} and Pd {Au} catalysts used for benzyl alcohol oxidation and hydrogen peroxide. Faraday Discussions, 152 (2011) 63-86.

[53] J. Pritchard, M. Piccinini, R. Tiruvalam, Q. He, N. Dimitratos, J.A. Lopez-Sanchez, D. J. Morgan, A.F. Carley, J.K. Edwards, C.J. Kiely, G.J. Hutchings, Effect of heat treatment on Au–Pd catalysts synthesized by sol immobilisation for the direct synthesis of hydrogen peroxide and benzyl alcohol oxidation. Catalysis Science & Technology 3 (2013) 308-317.

[54] R-Y. Zhong, K-Q. Sun, Y-C. Hong, B-Q. Xu, Impacts of Organic Stabilizers on Catalysis of Au Nanoparticles from Colloidal Preparation. ACS Catal. 4 (2014) 3982–3993.

[55] E.K. Gibson, A.M. Beale, C.R.A. Catlow, A. Chutia, D. Gianolio, A. Gould, A. Kroner, K.M.H. Mohammed, M. Perdjon, S.M. Rogers, P.P. Wells, Restructuring of AuPd nanoparticles studied by a combined XAFS/DRIFTS approach. Chemistry of Materials 27 (2015) 3714-3720.

[56] S. Solmi, C. Morreale, F. Ospitali, S. Agnoli, F. Cavani, Oxidation of d- Glucose to Glucaric Acid Using Au/C Catalysts. Chemcatchem 9 (2017) 2797-2806.

[57] N. Agarwal, S.J. Freakley, R.U. McVicker, S.M. Althahban, N. Dimitratos, Q. He, D.J. Morgan, R.L. Jenkins, D.J. Willock, S.H. Taylor, C.J. Kiely, G.J. Hutchings,

Aqueous Au-Pd colloids catalyze selective CH_4 oxidation to CH_3OH with O_2 under mild conditions. Science 358 (2017) 223-227.

[58] L.M. Rossi, J.L. Fiorio, M.A.S. Garcia, C.P. Ferraz, The role and fate of capping ligands in colloidally prepared metal nanoparticle catalysts. Dalton Trans. 47 (2018) 5889-5915.

[59] F. Sanchez, D. Motta, A. Roldan, C. Hammond, A. Villa, N. Dimitratos, Hydrogen generation from additive-free formic acid decomposition under mild conditions by Pd/C: Experimental and DFT studies. Top. Catal. 61 (2018) 254-266.

[60] M. Sankar, Q. He, R.V. Engel, M.A. Sainna, A.J. Logsdail, A. Roldan, D.J. Willock, N. Agarwal, C.J. Kiely, G.J. Hutchings, Role of the support in gold-containing nanoparticles as heterogeneous catalysts, Chem. Rev. 120 (2020) 3890-3938.

[61] S.J. Freakley, N. Dimitratos, D.J. Willock, S.H. Taylor, C.J. Kiely, G.J. Hutchings, Methane oxidation to methanol in water, Acc. Chem. Res. 54 (2021) 2614-2623.

[62] N. Yang, S. Pattisson, M. Douthwaite, G. Zeng, H. Zhang, J. Ma, G.J. Hutchings, Influence of Stabilizers on the Performance of Au/TiO_2 Catalysts for CO Oxidation. ACS Catal. 11 (2021) 11607-11615.

[63] S. Scurti, E. Monti, E. Rodríguez-Aguado, D. Caretti, J.A. Cecilia, N. Dimitratos, Effect of Polyvinyl Alcohol Ligands on Supported Gold Nano-Catalysts: Morphological and Kinetics Studies. Nanomaterials 11 (2021) 879–897.

[64] E. Monti, A. Ventimiglia, C.A. Garcia Soto, F. Martelli, E. Rodríguez-Aguado, J.A. Cecilia, A. Sadier, F. Ospitali, T. Tabanelli, S. Albonetti, F. Cavani, R. Wojcieszak, N. Dimitratos, Effect of the Colloidal Preparation Method for Supported Preformed Colloidal Au Nanoparticles for the Liquid Phase Oxidation of 1,6-Hexanediol to Adipic Acid. Catalysts 12 (2022) 196.

[65] J.A. Cecilia, C.P. Jiménez-Gómez, V. Torres-Bujalance, C. García-Sancho, R. Moreno-Tost, P. Maireles-Torres, Oxidative Condensation of Furfural with Ethanol Using Pd-Based Catalysts: Influence of the Support. Catalysts 10 (2020) 1309.

[66] J.A. Cecilia, L. Machogo, V. Torres-Bujalance, C.P. Jiménez-Gómez, C. García-Sancho, R. Moreno-Tost, P. Maireles-Torres, R. Luque, PdO Supported on TiO_2 for the Oxidative Condensation of Furfural with Ethanol: Insights on Reactivity and Product Selectivity. ACS Sustainable Chem. Eng. 9 (2021) 10100−10112.